

SUPPLEMENTAL MATERIAL

Impaired atrial mitochondrial calcium handling in patients with atrial fibrillation

Julius Ryan D. Pronto, PhD^{1,2}, Fleur E. Mason, PhD^{1,2}, Eva A. Rog-Zielinska, PhD³, Funsho E. Fakuade, PhD^{1,2,4}, Donata Bülow¹, Marcell Tóth⁵, Khaled Machwart, MD^{6,7}, Paulina Brandes¹, Felix Wiedmann, MD^{2,8,9,10}, Michael Kohlhaas, PhD⁷, Alexander Nickel, PhD⁷, Matthias Wolf¹¹, Julian Mustroph, MD^{11,12}, Kim-Chi Vu^{4,8,13}, Sören Brandenburg, MD^{4,8,13}, Tri Q. Do, PharmD¹⁴, Peter Joshua Siedler^{1,2}, Katharina Ritzenhoff^{1,2}, Zongqian Xue, MD^{10,15}, Xiaobo Zhou, MD^{10,15}, Stefanie Kestel^{1,2}, Olga Dschun¹⁶, Oksana Kyshynska¹⁷, George Kensah, PhD^{2,17}, Robyn T. Rebbeck, PhD¹⁸, Aschraf El-Essawi, MD^{2,17}, Ahmad Fawad Jebran, MD^{2,17}, Bernhard C. Danner, MD^{2,17}, Hassina Baraki, MD^{2,17}, Johann Schredelseker, PhD^{19,20}, Ivan Bogeski, MD²¹, Bianca J.J.M. Brundel, PhD²², Stephan E. Lehnart, MD^{2,4,8,13}, Constanze Bening, MD^{6,7,27}, Ingo Kutschka, MD^{2,17}, Felix Bremmer, MD¹⁶, Stefan M. Kallenberger, MD^{23,24}, Silvio O. Rizzoli, PhD^{4,25}, Björn C. Knollmann, MD¹⁴, Stefan Neef, MD¹¹, Katrin Streckfuss-Bömeke, PhD^{5,26}, Constanze Schmidt, MD^{2,8,9,10}, Christoph Maack, MD^{7,†}, Niels Voigt, MD^{1,2,4,†}

- ¹ Institute of Pharmacology and Toxicology, University Medical Center Göttingen, Germany
- ² DZHK (German Centre for Cardiovascular Research), partner site Lower Saxony, Göttingen, Germany
- ³ Institute for Experimental Cardiovascular Medicine (IEKM), University Heart Center and Faculty of Medicine, University of Freiburg, Germany
- ⁴ Cluster of Excellence "Multiscale Bioimaging: From Molecular Machines to Networks of Excitable Cells" (MBExC), Georg-August-University Göttingen, Germany
- ⁵ Institute of Pharmacology and Toxicology, Julius Maximilian University of Würzburg, Würzburg, Germany
- ⁶ Department of Thoracic and Cardiovascular Surgery, University Clinic Würzburg, Germany
- ⁷ Comprehensive Heart Failure Center Würzburg, University Clinic Würzburg, Germany
- ⁸ Department of Cardiology and Pneumology, University Medical Center Göttingen, Germany
- ⁹ Department of Cardiology, Angiology and Pneumology, University Hospital Heidelberg, Germany
- ¹⁰ DZHK (German Centre for Cardiovascular Research), partner site Heidelberg/Mannheim, Heidelberg, Germany
- ¹¹ Department of Internal Medicine II, University Hospital Regensburg, Regensburg, Germany
- ¹² Department of Pharmacology, University of Regensburg, Germany
- ¹³ Heart Research Center Göttingen, University Medical Center Göttingen, Göttingen, Germany
- ¹⁴ Department of Medicine, Vanderbilt University Medical Center, Nashville, Tennessee, USA
- ¹⁵ Department of Cardiology, Angiology, Hemostaseology and Medical Intensive Care, Medical Faculty Mannheim, Heidelberg University, Mannheim, Germany
- ¹⁶ Institute of Pathology, University Medical Center Göttingen, Göttingen, Germany
- ¹⁷ Department of Thoracic and Cardiovascular Surgery, University Medical Center Göttingen, Germany
- ¹⁸ Department of Biochemistry, Molecular Biology and Biophysics, University of Minnesota, Minneapolis, Minnesota, USA

- ¹⁹Walther Straub Institute of Pharmacology and Toxicology, Faculty of Medicine, LMU Munich, Munich
- ²⁰DZHK (German Centre for Cardiovascular Research), Partner Site Munich Heart Alliance, Munich, Germany
- ²¹Molecular Physiology, Institute of Cardiovascular Physiology, University Medical Center Göttingen, Germany.
- ²²Department of Physiology, Amsterdam UMC, Location Vrije Universiteit, Amsterdam Cardiovascular Sciences, Heart Failure and Arrhythmias, Amsterdam, The Netherlands.
- ²³Health Data Science Unit, University Hospital Heidelberg and Center for Quantitative Analysis of Molecular and Cellular Biosystems (BioQuant), University of Heidelberg, Heidelberg, Germany
- ²⁴National Center for Tumor Diseases, Department of Medical Oncology, Heidelberg University Hospital, Heidelberg, Germany
- ²⁵Department of Neuro- and Sensory Physiology, University Medical Center Göttingen, Germany
- ²⁶Medical Clinic I, Cardiology and Angiology, Justus-Liebig-University, Giessen
- ²⁷Current address: Rhein-Neckar Praxis, Eberbach, Germany
- [†] These authors share senior authorship.

Correspondence to:

Niels Voigt, Institute of Pharmacology and Toxicology, University Medical Center Göttingen, Robert-Koch-Straße 40, 37075 Göttingen, Germany. Phone: 0049-551-39-65174, E-mail: niels.voigt@med.uni-goettingen.de. X: @niels_voigt

Christoph Maack, Comprehensive Heart Failure Center (CHFC), University Clinic Würzburg, Am Schwarzenberg 15, Haus A15, 97078 Würzburg, Germany. Phone: +49-931-201-46502, E-mail: maack_c@ukw.de. X: @ChristophMaack

Supplemental Table S2. Characteristics of patients contributing atrial samples for mitochondrial respiration assay.....	22
Supplemental Table S3. Characteristics of patients contributing atrial tissue for Ca^{2+} sequestration assay.	23
Supplemental Table S4. Characteristics of patients contributing atrial samples for immunofluorescence and STED imaging.	24
Supplemental Table S5. Characteristics of patients contributing atrial myocytes for intracellular sodium measurements.	25
Supplemental Table S6. Characteristics of patients contributing atrial samples for immunoblotting.	26
Supplemental Table S7. Ezetimibe registry: demographic and clinical features of patients without ezetimibe treatment	27
Supplemental Table S8. Ezetimibe registry: demographic and clinical features of patients who initiated ezetimibe during follow-up (FU)	29
Supplemental Table S9. AF burden of patients before and after onset of ezetimibe therapy.	31
Supplemental Table S10. Antibodies used for immunofluorescent staining	31
Supplemental Table S11. Antibodies used for immunoblots	32
SUPPLEMENTAL STATISTICAL TABLE.....	33
Supplemental Figures.....	46
Supplemental Figure S1. Impaired oxidation of NADH and FADH_2 contributes to their accumulation which limits the activity of the tricarboxylic acid cycle.....	46
Supplemental Figure S2. Cytosolic and mitochondrial Ca^{2+} levels at increased stimulation frequencies in the absence of beta-adrenergic stimulation.....	47
Supplemental Figure S3. Coupling efficiency between $\text{I}_{\text{Ca,L}}$ and cytosolic Ca^{2+} transients in a porcine AF model under increased workload.	49
Supplemental Figure S4. Na^+ homeostasis in atrial myocytes from control (Ctrl) and atrial fibrillation (AF) patients.....	50

Supplemental Figure S5. Expression of SR-mitochondria tethering and mitochondrial dynamics proteins previously implicated in mitochondrial Ca^{2+} handling is unchanged. ...	51
Supplemental Figure S6. MitoTEMPO has no effect on Ca^{2+} sparks in control atrial hiPSC-CMs.	52
Supplemental Figure 7. Ezetimibe increased mitochondrial Ca^{2+} levels and rescues against Ca^{2+} sparks in hiPSC-CMs.	53
Supplemental Figure 8. Ezetimibe has no effect on cytosolic Ca^{2+} transient decay.	54
Supplemental Figure S9. Ezetimibe effects on RyR2 single-channel recordings.	55
Supplemental Figure S10: Protein expression and phosphorylation status of RyR2 in atrial human induced pluripotent stem cell-derived cardiac myocyte (hiPSC-CM) treated with ezetimibe.	56
Supplemental Figure S11. Percentage change of peak L-type Ca^{2+} current during 0.5 Hz stimulation.	57
Supplemental Figure S12. Validation of VDAC antibody used for STED imaging.	58

Supplemental Methods

All protocols were approved by the Ethics Committee of the University Medical Center Göttingen (No. 10/9/15, 15/2/20 and No. 4/11/18). Informed consent was obtained from all participants and all research was performed in accordance with relevant guidelines and regulations.

Patients

Experimental protocols were approved by the ethics committee of the University Medical Center Göttingen (Ethics Approval No.4/11/18), the University Clinic Würzburg (Ethics Approval No. 143/17-sc) and the University Medical Center Regensburg (Ethics Approval No. 22-2802-101). Patients in sinus rhythm (control, Ctrl) and long-term persistent atrial fibrillation (AF) qualified for this project (electrophysiological experiments, isolated mitochondria assay and tissue structure analysis).

For the retrospective study on ezetimibe use, patients were identified at the University Hospital Heidelberg (Ethics Approval S-756/2022), who presented for an implanted cardiac device interrogation during the period 2015-2020 and who were initiated on ezetimibe therapy. Inclusion criteria were patient age ≥ 18 years and the presence of a dual-chamber pacemaker, a defibrillator system or a cardiac resynchronization therapy (CRT) device that can accurately determine the paroxysmal AF burden. Exclusion criteria included catheter ablation or initiation of antiarrhythmic therapy within a 12 month time frame before or after initiation of ezetimibe therapy and the presence of persistent AF. Ethnicity was not assessed in the patient population. Patient group size was determined by the availability of continuous device monitoring before and after ezetimibe initiation; no a priori power calculation was performed. Instead, a within-patient pre-post analysis design was employed, which enhanced robustness despite the limited cohort size. All included patients were male, reflecting the available clinical population

fulfilling the strict inclusion criteria. We acknowledge that sex differences could not be addressed in this cohort, which is an inherent limitation of the study.

Patch-clamp experiments to increase cellular workload

Atrial myocytes were isolated from the right atrial appendage of patients (**Supplemental Table S1**) undergoing cardiac surgery, as previously described.²³ All simultaneous patch-clamp and fluorescence recordings were performed in parallel on an inverted fluorescence microscope (Olympus IX73, Olympus, Japan) and performed at 37 °C. All acquired signals from the photon multiplier tubes (PMT) and the headstage were digitized via Digidata 1550B and visualized in Clampex 10.7 software (all from Axon Instruments, Molecular Devices, CA, USA). Digitized data were acquired at a sampling rate of 10 kHz.

Myocytes were transferred to a 37 ± 0.5 °C heated chamber and were superfused with modified Tyrode's solution (bath solution, in mmol/L: NaCl 140; KCl 4; MgCl₂ 1; HEPES 10; Glucose 10; CaCl₂ 2; Na-pyruvate 2; Ascorbic acid 0.3; 4-aminopyridine 5; BaCl₂ 0.1; pH = 7.35 adjusted with NaOH). Myocytes were patched in the whole-cell ruptured-patch configuration and voltage clamp was applied to elicit L-type Ca²⁺ current, I_{Ca,L} (holding potential -80 mV, 100 ms ramp pulse to -40 mV to inactivate the fast Na⁺ current, 100 ms depolarizing voltage step to 10 mV). Monitoring of L-type Ca²⁺ peak density during 0.5 Hz stimulation showed no considerable rundown (**Supplemental Figure S11**). Stimulation rate was 0.5 Hz at baseline, during which an initial baseline measurement was recorded. To simulate workload transitions, myocytes were subjected to increased stimulation frequency (3 Hz), and further β-adrenergic stimulation (100 nmol/L isoproterenol, ISO, in bath solution) during 3 Hz. This was followed by a washout step (bath solution) at 0.5 Hz stimulation. All stimulation frequencies were applied in series on each cell. Pipette solution contained, in mmol/L: K-Glutamate 130; KCl 19; Na-HEPES 5; MgCl₂ 0.5; Mg-ATP 5; HEPES 10; pH = 7.2 adjusted with KOH.

Membrane currents were measured and analyzed using pClamp-Software (Molecular Devices 10.7). Tip resistance of borosilicate glass microelectrodes was 3-7 M Ω . Membrane capacitance measurements were acquired and current was expressed as current density (pA/pF).

NAD(P)H and FAD autofluorescence measurement

To determine redox index, NAD(P)H and FAD autofluorescence signals were measured during workload transition experiments (see above). Myocytes were alternately excited (150 ms) with LEDs: 365 nm for NAD(P)H and 470 nm FAD. Emissions were collected at 435 nm for NAD(P)H and at 545 nm for FAD. Emissions were collected every 4 s. To calibrate NAD(P)H and FAD recordings, FCCP (5 μ mol/L) and Na-cyanide (4 mmol/L) in bath solution were washed in consecutively at the end of each experiment (in the absence of stimulation), causing maximum oxidation and reduction, respectively, as previously described.² NAD(P)H/FAD ratio was used to report redox index.

Mitochondrial and cytosolic Ca²⁺ transient measurement

Mitochondrial Ca²⁺ ([Ca²⁺]_m) and cytosolic Ca²⁺ ([Ca²⁺]_c) were measured simultaneously during the workload transition protocol (see above). Myocytes were incubated with 5 μ mol/L Rhod-2 AM (R1245MP, Invitrogen) for 1 h in bath solution (see above, omitting 4-aminopyridine 5; BaCl₂ 0.1), followed by 1 h de-esterification in Rhod-2-free solution, both at at 37 °C. Rhod-2 AM accumulates primarily in the mitochondria due to its positive charge. Cytosolic Ca²⁺ was labeled with 75 μ mol/L Indo-1 pentapotassium salt (21040, AAT Bioquest); this was loaded into the cytosol via the patch pipette for 6 min prior to each experiment, thereby dialyzing any cytosolic traces of Rhod-2, as previously described.²⁹ Indo-1 was excited with a 340 nm LED and emissions were collected at 405 nm (F₄₀₅, Ca²⁺-bound) and 480 nm (F₄₈₀, Ca²⁺-unbound). Rhod-2 was excited with a white light and a 545/25x clean-up filter and emissions were collected at 605 nm. The same workload transition protocol (increased

stimulation frequency \pm ISO) applied during NAD(P)H/FAD measurements was used and average Ca^{2+} handling parameters were analyzed.

Current clamp and measurement of APs, SCAEs and DADs

Action potentials (APs), spontaneous Ca^{2+} release events (SCAEs) and concomitant delayed afterdepolarizations (DADs) were detected using current-clamp in whole-cell ruptured-patch configuration. AF myocytes were incubated with 10 $\mu\text{mol/L}$ Fluo-3 AM in bath solution for 10 min at room temperature, followed by a de-esterification step with indicator-free bath solution for 30 min. Myocytes were treated either with 1 $\mu\text{mol/L}$ ezetimibe in DMSO (0.01 %) or DMSO alone (control) for 30 min. Fluo-3-loaded myocytes were then stimulated at 0.5 Hz and APs were triggered by injection of 1 ms long current pulses increasing in 1 nA increments. APs were recorded at 1.2-1.5x the current pulse where an AP was initially observed. No series resistance compensation was applied. 1 min of 0.5 Hz stimulation was followed by 1 min observation at resting membrane potential. To calibrate the fluorescence signal, recordings were converted to Ca^{2+} concentration based on the *in vivo* K_d of Fluo-3 at 37 °C (864 nM). SCAEs and DADs traces were transferred to Labchart where frequency and amplitude of SCAEs and DADs were quantified.

Mitochondria isolation

Left atrial mitochondria were isolated from Ctrl and AF patients (**Supplemental Table S3**) undergoing open heart surgery following previously established protocols.³ All media were ice-cold and all steps were performed on ice or at 4 °C. The atrial samples were transferred into a 2 mL tube with 500 μL isolation solution containing (in mmol/L): mannitol 225, sucrose 75, HEPES 2, EGTA 1, Nagarse 0.16 mg/mL (pH 7.4). The tissue was cut and minced with scissors and subsequently transferred to a 5 mL homogenizer (Teflon pestle) and manually homogenized in 1 mL isolation solution for 14 min. The homogenate was centrifuged at low speed (400 x g)

in a pre-cooled (4 °C) centrifuge for 5 min to remove cell debris. The supernatant obtained from the first centrifugation was centrifuged at high speed (7,700 x g) for 10 min, and the pellet - containing mitochondria - was washed in 1 mL mitochondrial suspension solution containing (in mmol/L): mannitol 225, sucrose 75, HEPES 2 (pH 7.4), and centrifuged again twice at high speed (7700 g) for 10 min. The pellet obtained from the final centrifugation step was resuspended in 100-150 µL mitochondrial suspension solution and used for experiments.

Oxygen consumption measurements

Atrial cardiac mitochondria were isolated as described previously.⁸³ Oxygen consumption was detected at 37 °C with an Oxygraph-2k high-resolution respirometer (Oroboros Instruments, Innsbruck, Austria) and Smart Fluoro-Sensor Green, using 800 µg of isolated mitochondria diluted in 2.1 mL standard respiration buffer containing (in mmol/L): KCl 137, KH₂PO₄ 2, EGTA 0.5, MgCl₂ 2.5, HEPES 20, at pH 7.2. Measurement of complex I activity was performed with 5 mmol/L Na-pyruvate and 5 mmol/L Na-malate, and 1 mmol/L ADP was added to induce maximal state 3 respiration. Complex I was inhibited by 0.5 µmol/L rotenone to prevent reverse electron flux. Patient characteristics for the samples used for oxygen consumption measurements are listed in **Supplemental Table S2**.

Mitochondrial Ca²⁺-retention capacity

Mitochondrial Ca²⁺ uptake was measured as previously described.³⁰ Ca²⁺ retention capacity of isolated mitochondria was determined by exposing mitochondria to repeated Ca²⁺ pulses (final free Ca²⁺ concentration 10 µmol/L each pulse) and simultaneously measuring extramitochondrial Ca²⁺ levels with the fluorescent indicator Calcium Green-5N (C3737, Invitrogen). using a fluorescence plate reader (Infinite M200Pro, Tecan). Calcium Green-5N was excited at 503 nm and emissions were collected at 535 nm. The assay was performed at 37 °C in a 96-well transparent bottom plate. The experiment was conducted in PTP buffer

containing (in mmol/L): KCl 120, mannitol 70, sucrose 25, HEPES 20, KH₂PO₄ 5, EGTA 0.02. For each replicate, 165 µg mitochondria were dissolved in 200 µL PTP buffer. Mitochondria were incubated with potassium glutamate (5 mmol/L), sodium malate (2.5 mmol/L), and the mPTP inhibitor cyclosporine A (2 µmol/L) for 5 min. Calcium Green-5N (1 µmol/L) was added immediately before starting the experiment. The amount of Ca²⁺ required to obtain 10 µmol/L free Ca²⁺ for each addition was calculated with Maxchelator (RRID:SCR_000459).⁸⁴ Patient characteristics for the samples used for Ca²⁺ retention capacity experiments are listed in **Supplemental Table S3**.

Electron tomography and 3D segmentation

Atrial appendages were immediately transferred to vials with Karnovsky fixative (HST408S-C, Solmedia, UK). Preparations underwent processing as described before,⁸⁵ and were imaged using a transmission electron microscope (Tecnai TF30, FEI, Eindhoven, The Netherlands) operating at 300 kV. For 3D data acquisition, tilt-series were acquired from +60° to -60° at 1° intervals. The images were aligned to generate a 3D reconstruction of the original partial cell volume. All tomograms were processed and analyzed using IMOD software.⁵

Immunofluorescence staining

Right atrial appendages were transferred from the transport solution to 4% PFA for 24-48 h. Depending on fixation time, tissues were soaked in water for 3-4 h and were then embedded on paraffin. Tissue sections 0.5-1 µm thickness were cut with a S35 blade mounted to a sliding microtome (Leica SM 2000R, Leica Biosystems, Germany). Sections were then transferred onto cold water and then allowed to expand on 45 °C water before mounting onto glass slides. The tissue sections were deparaffinized at 60 °C for 1-2 h in an oven (Mettt UNB200) before performing an antigen retrieval step with 1X EnVision FLEXTarget Retrieval Solution, High pH (K8004, Agilent Dako) for 15 min at 97 °C with a PT Link PT200 Autostainer (Agilent

Dako), and kept in 1X EnVision FLEX Wash Buffer (K8007, Agilent Dako) until further processing. The surrounding of the tissue section was dried and an oval perimeter around the tissue was drawn using a hydrophobic pen. The sections were blocked and permeabilized with blocking buffer containing 1% BSA and 0.1% Triton-X-100 in PBS for 1 h, followed by incubation with primary antibodies diluted in blocking buffer overnight at 4 °C. After washing blocking buffer, the sections were then incubated with secondary antibodies in blocking buffer for 2 h at room temperature in the dark. #1.5 cover slips (160-190 µm) were mounted with Mowiol. All antibodies used are listed in **Supplemental Table S11**. Specificity of immunostaining was validated by secondary antibody-only controls, which yielded no detectable signal. Patient characteristics for the samples used for immunofluorescence experiments are listed in **Supplemental Table S4**.

Confocal and STED imaging

A Leica TCS SP8 system with a HC PL APO C2S 100x/1.40 oil objective was used for dual-color STED or confocal imaging. Type-F immersion liquid (all from Leica Microsystems, Germany) was used during experiments. Using the Leica Application Software (LAS-X), the following parameters were assigned: pixel size 114 nm x 114 nm (16 x 16 nm for STED), 1024 x 1024 pixel image, 200 Hz sampling rate, 16x line averaging. STAR 580 and MitoTracker Orange CMTMRos were excited at 580 nm and emissions were collected at 600-630 nm and STAR 635P was excited at 635 nm and emissions were collected at 650-700 nm. For STED, depletion of both fluorophores was achieved via a 775 nm laser beam. STED images were acquired at 200 Hz. Raw images were processed in Fiji (<https://imagej.net/Fiji>).

MATLAB (MathWorks, US) was used for colocalization using Ripley *K* curve and statistical analyses. TIFF images were opened in MATLAB. RyR2 spots were designated as reference particles, with which the degree of aggregation of VDAC spots within an assigned radius was

measured. ROI was assigned arbitrarily, avoiding perinuclear regions. Thresholding was performed by spot erosion and dilation. Centroids of each spot were extrapolated and used for distance measurements. The analysis program generated a line scan profile from the averaged spots. Signal was normalized to baseline (points 8 to 16) and a two-way ANOVA was performed on the first 10 points.

For the nearest neighbor analysis, centroid-to-centroid Euclidean distance was calculated from thresholded and binarized images using Fiji (<https://imagej.net/Fiji>).

Quantification of observed microtubule morphologies was done based on the visual appearance of microtubules: filamentous, sarcomeric or disintegrated. All images were pooled, randomized, and then renamed using a batch file renaming software (<https://www.advancedrenamer.com/>). Based on microtubule appearance, all images were manually classified into three distinct categories reflecting morphological phenotypes mentioned above, and then later quantified for both Ctrl and AF groups.

Intracellular sodium measurement

Atrial cardiac myocytes were isolated from tissue slices, previously described.⁸⁶ Intracellular Na⁺ levels were assessed using the ratiometric Na⁺-sensitive dye sodium-binding benzofuran isophthalate-acetoxymethyl ester (10 μmol/L SBFI-AM, S1264, Invitrogen) as previously described.⁸⁷ Cells were incubated with the dye for 90 min at 37 °C, followed by a 20 min de-esterification period in modified Tyrode's solution at the same temperature (in mmol/L: 140 NaCl, 4 KCl, 1 MgCl₂, 10 HEPES, 10 glucose, and 2 CaCl₂, pH 7.4 with NaOH). For fluorescence recordings, cells were mounted on an inverted microscope equipped with a fluorescence detection system (IonOptix) and field-stimulated at 30 and 180 bpm to maintain steady-state Na⁺ concentrations. Emission was recorded at 510 ± 40 nm following alternating excitation at 340 and 380 nm. Each cell was recorded for 3 s under steady-state conditions.

Patient characteristics for the samples used for sodium measurements are listed in **Supplemental Table S5**.

Immunoblotting

Protein isolation and immunoblotting of LN₂-frozen atrial tissues and atrial hiPSC-CMs were performed as previously described^{10,11}. Signals were visualized using a fluorescence and chemiluminescence (Thermo Fisher) imaging system (Odyssey CLx, LI-COR), respectively. Image Studio Software (LI-COR) was used for quantification. Protein expression was normalized to total protein load as indicated by REVERT™ total protein staining (LI-COR Biotechnology, USA) or GAPDH. Primary and secondary antibodies are listed below in **Supplemental Table S11**. Total protein staining images are shown in **Unedited Immunoblots**. Patient characteristics for the samples used for immunoblotting are listed in **Supplemental Table S6**.

Simultaneous measurements of I_{Ca,L} and cytosolic Ca²⁺ transients in atrial myocytes from a pig model of atrial fibrillation

The translational model of AF established at the Heidelberg site uses male domestic pigs (~3 months old, 45–55 kg). Male animals were selected because they are less prone to stress-related sudden death and malignant cardiac arrhythmias, which may otherwise compromise feasibility and reproducibility. All animal experiments were conducted in accordance with the Guide for the Care and Use of Laboratory Animals adopted by the US National Institutes of Health (NIH publication No. 86-23, revised 1985), with EU Directive 2010/63/EU, with the current version of the German Law on the Protection of Animals, and the ARRIVE guidelines. The study protocol was approved by the local Animal Welfare Committee (Regierungspräsidium Karlsruhe, Germany, reference numbers G-67/20). After induction of anaesthesia, the pigs undergo basic cardiac diagnostics and an invasive electrophysiological examination to measure

arrhythmia inducibility. A dual-chamber pacemaker system is implanted and AF is induced by atrial burst pacing (40 Hz)^{89,90}. To prevent development of arrhythmia-induced cardiomyopathy, atrioventricular node ablation was performed under fluoroscopic guidance. After a 2-week experimental period, basic diagnostics and invasive studies are repeated, followed by organ extraction and further processing of atrial tissue samples. This study was conducted in an exploratory manner to support the primary experimental hypothesis and to reproduce the observations in an animal disease model. Consequently, no formal sample size calculation was undertaken. Instead, the findings were confirmed in three independent animals per group. Neither randomization nor blinding were applied.

Atrial myocytes from pigs were isolated as previously described.⁹¹ Please refer to human atrial isolation for details. Atrial myocytes were incubated with Fluo-3 AM (21013, AAT Bioquest) for 10 min, followed by a de-esterification step in indicator-free Tyrode buffer. Whole-cell ruptured voltage clamp experiments on pig atrial myocytes were performed similarly to those on human atrial myocytes, except for pipette resistance being 5–7 MΩ. Additionally, Fluo-3 pentapotassium salt (21017, AAT Bioquest) was added to the pipette solution. Fluo-3 was excited at 488 nm, and emission above 520 nm was recorded. Intracellular calcium concentration ($[Ca^{2+}]_i$) was calculated using the formula:

$$[Ca^{2+}]_i = K_d \left(\frac{F}{F_{max} - F} \right)$$

where $K_d=864$ nM, F is the fluorescence intensity, and F_{max} represents the fluorescence at calcium saturation, determined at the end of each experiment. Calcium transients were analyzed by averaging 5 consecutive traces.

RyR2 single-channel recordings

The use of animals was approved by the Institutional Animal Care and Use Committee of the University of Minnesota (Protocol #2301-40726A).

Pig heart muscle was minced and homogenized in a Waring blender (4 x 15 s bursts) in homogenizing buffer containing 0.3 mol/L sucrose, 10 mmol/L imidazole, 0.5 mmol/L phenylmethylsulfonylfluoride (PMSF), 1 µg/mL leupeptin, 1 µg/mL pepstatin A, 1 mmol/L benzamidine, 0.5 mmol/L dithiothreitol (DTT), 3 mmol/L NaN₃, and 20 mmol/L NaF, pH 6.9, followed by 10 manual strokes of a loose-fitting glass/glass Dounce homogenizer. The homogenate was centrifuged at 8,000 x g for 20 min using a Beckman Optima L-100XP Ultracentrifuge. The supernatant was then centrifuged at 170,000 x g for 30 min. The resultant pellet was resuspended with homogenizing buffer containing 0.65 mol/L KCl using a glass/glass Dounce homogenizer, incubated for 30 min on ice and then centrifuged at 8,000 x g for 15 min. The supernatant was centrifuged at 170,000 x g for 1 h, and the resulting microsomes from the pellet were resuspended in storage buffer (homogenizing buffer + 0.65 mol/L KCl), snap-frozen in liquid nitrogen and stored at -80 °C.

All solutions were pH buffered using 10 mmol/L TES (N-tris[hydroxymethyl] methyl-2-aminoethanesulfonic acid; Sigma-Aldrich) and titrated to pH 7.4 using CsOH (ICN Biomedicals). Free Ca²⁺ of 100 nmol/L in the cis bath was generated from 1 mmol/L CaCl₂ and 4.5 mmol/L BAPTA (1,2-bis-(2-aminophenoxy)ethane-N,N,N',N'-tetraacetic acid ; Invitrogen) and this was validated using a Ca²⁺ electrode (ThermoFisher). To start the experiment, lipid bilayers were painted across an aperture with diameter 150-250 µm of a delrin cup using a lipid mixture of phosphatidylethanolamine, phosphatidylserine and phosphatidylcholine (5:3:2 wt/wt, Avanti Polar Lipids) in n-decane (50 mg/mL, ICN Biomedicals). During the SR vesicle fusion period, the cis (cytoplasmic) chamber contained 250 mmol/L Cs⁺ (230 mmol/L CsCH₃O₃S, 20

mmol/L CsCl) + 1 mmol/L CaCl₂ and the trans (luminal) chamber contained 50 mmol/L Cs⁺ (30 mmol/L CsCH₃O₃S, 20 mmol/L CsCl) + 1 mmol/L CaCl₂. When ion channels were detected in the bilayer, the trans Cs⁺ was raised to 250 mmol/L by aliquot addition of 4 mol/L CsCH₃O₃S. During experiments, the composition of the cis solution was altered by a perfusion system and the trans solution was altered by aliquot additions. Experiments were carried out at room temperature (23 ± 2 °C).

RyR2 single channel analysis

Electric potentials are expressed using standard physiological convention (i.e. cytoplasm relative to SR lumen at virtual ground). Control of the bilayer potential and recording of unitary currents was done using an Axopatch 200B amplifier (Axon Instruments, Molecular Devices, CA, USA). Channel currents were digitized at 20 kHz and low pass filtered at 5 kHz. Before analysis the current signal was re-digitized at 5 kHz and low pass-filtered at 1 kHz. Individual readings of open probability were derived from 30-60 s of RyR2 recording. Single channel open probability was measured using a threshold discriminator at 50% of channel amplitude (Channel3, nic@niclaver.com.au). Open probabilities from multi-channel recording were calculated from the ratio of the mean current and unitary current. Dwell time analysis (mean open time – T_o and mean closed time – T_c) were done when there was only 1 channel in the bilayer.

Generation of hiPSC-CMs

Fibroblasts/peripheral blood cells from patients were reprogrammed using a Sendai-based induction protocol, as previously described.⁹² Differentiation of hiPSCs into cardiac myocytes was initiated by mesoderm induction, Wnt inhibition, and subsequent metabolic selection with glucose-free, lactate-supplemented media.⁹² hiPSC-derived cardiac myocytes (hiPSC-CMs) were allowed to mature in Cardio Culture Medium containing RPMI-Glutamax (618-70010,

Gibco) and B27 supplement (17504044, ThermoFischer) up to day 75 prior to experimental use.

Mitochondrial Ca^{2+} measurement in iPSC-CM

Mitochondrial Ca^{2+} imaging was performed by using the confocal Nikon microscope. 300,000 iPSC-CMs were seeded on Geltrex-coated 35mm glass-bottom dishes (MatTek). 7 days after plating, transfection of 1 μg ratiometric mito Pericam-GFP plasmid³⁹ was performed using Lipofectamine LTX Reagent with PLUS (15338100, Invitrogen) according to the manufacturers' instructions.

3 days after transfection, measurements were performed using a 40x objective Nikon ECLIPSE Ti2, a Nikon AX R Galvano scan head, and a Tokaihit warming box. 1 $\mu\text{mol/L}$ Ezetimibe (74798364, Molekula) was added for 30 min, and 10 $\mu\text{mol/L}$ Nocodazole (HY-13520, MedChemExpress) for 1 h in Cardio Culture Medium directly before measurement. During measurement, cells were in Tyrode's solution containing 1.8 mM CaCl_2 (pH 7.4) under conditions of 37 °C, 5% CO_2 , and paced with 0.5 Hz using an IonOptix Myo Pacer Field stimulator. 1 $\mu\text{mol/L}$ Ezetimibe and/or 10 $\mu\text{mol/L}$ Nocodazole were added to the Tyrode's solution for 5 min before measurements. Excitation occurred at 405 nm and 488 nm, with signal detection at 420-515 nm and 499-541 nm.

The pictures were analyzed using Fiji. The ratio of the emission intensities at excitation with 488 nm and 405nm (488nm/405nm) was calculated and used as a value for mitochondrial Ca^{2+} concentration. All iPSC-CM were measured 75 days after the start of differentiation.

Immunofluorescence of hiPSC-derived cardiac myocytes

Atrial hiPSC-CMs were generated using an established protocol,⁹³ where supplementation with retinoic acid prior to lactate selection promoted atria-specific cardiac myocyte differentiation. hiPSC-CMs from at least day 60 of differentiation were seeded at a density of 30,000 cells per

coverslip onto 10 mm glass coverslips pre-coated with Matrigel (1:30) and cultured for at least a week. Cells were treated with either DMSO or 10 $\mu\text{mol/L}$ nocodazole with or without 1 $\mu\text{mol/L}$ ezetimibe for 1 h at 37 °C. To label mitochondria, cells were incubated with 500 nmol/L MitoTracker Orange CMTMRos (M7510, Invitrogen) for 30 min at 37 °C. Cells were then fixed in 4% paraformaldehyde for 15 min at 37 °C and washed three times in PBS. Permeabilization and blocking were performed for 1 h at room temperature using a blocking buffer with 1% bovine calf serum and 0.1% Triton X-100 in PBS. Cells were incubated overnight at 4 °C with a rabbit anti- β -tubulin primary antibody (1:75 in blocking buffer). The next day, coverslips were washed and incubated for 1 h at room temperature in the dark with abberior STAR 635P anti-rabbit IgG (1:200 in blocking buffer) and finally incubated with DAPI (1:15,000 in blocking buffer). After a final series of washes, coverslips were mounted using Mowiol mounting medium. Imaging was performed using a confocal microscope (Leica SP8) with a HC PL APO C2S 100x/1.40 oil objective. Fluorophores were excited at 550 nm (Mitotracker), 635 nm (β -tubulin), and 405 nm (DAPI), with emissions collected at 570–590 nm, 650–700 nm, and (420–476 nm), respectively. Raw images were processed in Fiji.

Mitochondrial network analysis

For mitochondrial analysis, mitochondrial regions of interest were analyzed using the Fiji plugin Mitochondrial Network Analysis (MiNA) toolset. The mitochondrial networks were quantified by calculating the percentage of objects in the image containing at least one junction pixel (indicating networks with multiple branches) relative to the total number of objects analyzed.

Ca²⁺ spark imaging

Atrial hiPSC-CMs cultured on Matrigel-coated coverslips (as described above) were loaded with 5 $\mu\text{mol/L}$ Fluo-4 AM (F14201, Invitrogen) in 20% pluronic acid (in DMSO) for 15 min at

37 °C. Following loading, cells were washed and incubated for an additional 15 min at 37 °C to allow for de-esterification. Coverslips were then transferred to a custom recording chamber perfused with modified Tyrode's solution (in mM: 140 NaCl, 5.4 KCl, 1 MgCl₂, 1.8 CaCl₂, 10 glucose, and 10 HEPES, pH 7.4 adjusted with NaOH). Electrical field stimulation at 1 Hz was applied using platinum electrodes mounted in the chamber and controlled via a MyoPacer stimulator (IonOptix, USA). Confocal imaging was performed using a Zeiss LSM 510 laser-scanning microscope equipped with a 63× oil immersion objective (numerical aperture = 1.4). Fluo-4 was excited using the 488 nm line of an argon laser, and emitted fluorescence was collected at wavelengths >505 nm. Line-scan images (512 × 1 pixels) were acquired at a scan speed of 1.52 ms per line for 10,000 consecutive lines. Spark detection was performed using SparkMaster2.⁹⁴

For all experiments performed on iPSC-derived cardiac myocytes, individual cells were treated as independent observations. This approach reflects previous observations that inter-cell heterogeneity is typically greater than batch-to-batch variation, as supported by prior work.⁹⁵

Supplemental Tables

Supplemental Table S1. Characteristics of patients contributing atrial myocytes for electrophysiological experiments

	Ctrl	AF
Patients, n	59	23
Sex, male/female	52/7	20/3
Age, y	64.3 ± 9.9	71.4 ± 7.2**
Body mass index, kg/m ²	28.4 ± 4.3	29.0 ± 4.5
CAD, n	38	15
MVD/AVD, n	11	7
CAD+MVD/AVD, n	10	1
Hypertension, n	53	16
Diabetes, n	13	9
Hyperlipidemia, n	29	9
ACE inhibitors, n	25	13
AT1 blockers, n	17	9
β-Blockers, n	38	20
Digitalis, n	0	1
Dihydropyridines, n	13	5
Diuretics, n	18	11
Lipid-lowering drugs, n	47	18
Nitrates, n	3	3

ACE, angiotensin-converting enzyme; AT, angiotensin receptor; CAD, coronary artery disease; LVEF, left ventricular ejection fraction; MVD/AVD, mitral/aortic valve disease. Continuous data are expressed as mean ± SD. n indicates number of patients. ** $P < 0.01$ vs. Ctrl. Comparisons were made using Student *t* test and Fisher's exact test for continuous and categorical data, respectively.

Supplemental Table S2. Characteristics of patients contributing atrial samples for mitochondrial respiration assay.

	Ctrl	AF
Patients, n	50	20
Sex, male/female	40/10	15 /5
Age, y	72 ± 12.6	75 ± 6.7
Body mass index, kg/m ²	27.1 ± 3.9	27.9 ± 2.8
CAD, n	50	20
Hypertension, n	41	15
Diabetes, n	13	2
Hyperlipidemia, n	26	9
LVEF, %	53 ± 4	48 ± 9
ACE inhibitors, n	20	10
AT1 blockers, n	16	7
β-Blockers, n	50	20
Digitalis, n	0	0
Dihydropyridines, n	13	5
Diuretics, n	18	11
Lipid-lowering drugs, n	35	9
Nitrates, n	0	0

ACE, angiotensin-converting enzyme; AT, angiotensin receptor; CAD, coronary artery disease; LVEF, left ventricular ejection fraction. Continuous data are expressed as mean ± SD. n indicates number of patients.

Supplemental Table S3. Characteristics of patients contributing atrial tissue for Ca²⁺ sequestration assay.

	Ctrl	AF
Patients, n	38	12
Sex, male/female	31/7	8/4
Age, y	67 ± 9	73 ± 9
Body mass index, kg/m ²	28.8 ± 5.1	27.4 ± 2.9
CAD, n	38	12
Hypertension, n	31	10
Diabetes, n	3	10
Hyperlipidemia, n	5	18
LVEF, %	55 ± 8	50 ± 6*
ACE inhibitors, n	20	6
AT1 blockers, n	11	3
β-Blockers, n	28	11
Digitalis, n	0	1
Dihydropyridines, n	12	5
Diuretics, n	9	7*
Lipid-lowering drugs, n	30	9
Nitrates, n	0	1

ACE, angiotensin-converting enzyme; AT, angiotensin receptor; CAD, coronary artery disease; LVEF, left ventricular ejection fraction. Continuous data are expressed as mean ± SD. n indicates number of patients. **P* < 0.05 vs. Ctrl. Comparisons were made using Student *t* test and Fisher's exact test for continuous and categorical data, respectively.

Supplemental Table S4. Characteristics of patients contributing atrial samples for immunofluorescence and STED imaging.

	Ctrl	AF
Patients, n	13	12
Sex, male/female	11/2	10/2
Age, y	64.9 ± 10.6	71.9 ± 7.9
Body mass index, kg/m ²	28.0 ± 3.9	29.8 ± 4.0
CAD, n	8	6
MVD/AVD, n	2	4
CAD+MVD/AVD, n	3	2
Hypertension, n	12	8
Diabetes, n	5	4
Hyperlipidemia, n	7	6
LVEF, %	56 ± 13	50 ± 9
ACE inhibitors, n	7	7
AT1 blockers, n	3	5
β-Blockers, n	8	10
Digitalis, n	0	1
Dihydropyridines, n	4	5
Diuretics, n	4	8
Lipid-lowering drugs, n	9	10
Nitrates, n	2	1

ACE, angiotensin-converting enzyme; AT, angiotensin receptor; CAD, coronary artery disease; LVEF, left ventricular ejection fraction; MVD/AVD, mitral/aortic valve disease. Continuous data are expressed as mean ± SD or individual values. n indicates number of patients.

Supplemental Table S5. Characteristics of patients contributing atrial myocytes for intracellular sodium measurements.

	Ctrl	AF
Patients, n	5	2
Sex, male/female	3/2	2/0
Age, y	65.8 ± 8.3	50, 62
Body mass index, kg/m ²	29.2 ± 5.2	33.3, 26.0
CAD, n	0	0
MVD/AVD, n	2	2
CAD+MVD/AVD, n	3	0
Hypertension, n	4	1
Diabetes, n	1	0
Hyperlipidemia, n	0	0
LVEF, %	55 ± 6	40, 50
ACE inhibitors, n	4	0
AT1 blockers, n	0	1
β-Blockers, n	4	1
Digitalis, n	0	1
Dihydropyridines, n	0	0
Diuretics, n	2	1
Lipid-lowering drugs, n	3	1
Nitrates, n	0	0

ACE, angiotensin-converting enzyme; AT, angiotensin receptor; CAD, coronary artery disease; LVEF, left ventricular ejection fraction; MVD/AVD, mitral/aortic valve disease. Continuous data are expressed as mean ± SD or individual values. n indicates number of patients.

Supplemental Table S6. Characteristics of patients contributing atrial samples for immunoblotting.

	Ctrl	AF
Patients, n	46	35
Sex, male/female	39/7	26/9
Age, y	62.6 ± 10.2	71.7 ± 7.9***
Body mass index, kg/m ²	28.1 ± 6.6	26.4 ± 4.0
CAD, n	39	18**
MVD/AVD, n	3	11**
CAD+MVD/AVD, n	4	6
Hypertension, n	37	29
Diabetes, n	11	12
Hyperlipidemia, n	20	15
LVEF, %	50 ± 14	50 ± 13
ACE inhibitors, n	24	16
AT1 blockers, n	9	10
β-Blockers, n	33	27
Digitalis, n	0	4*
Dihydropyridines, n	11	8
Diuretics, n	15	20**
Lipid-lowering drugs, n	36	21
Nitrates, n	2	0

ACE, angiotensin-converting enzyme; AT, angiotensin receptor; CAD, coronary artery disease; LVEF, left ventricular ejection fraction; MVD/AVD, mitral/aortic valve disease. Continuous data are expressed as mean ± SD or individual values. n indicates number of patients. **P*<0.05, ***P*<0.01, *** *P*<0.001 vs Ctrl. Comparisons were made using Student *t* test and Fisher's exact test for continuous and categorical data, respectively.

Supplemental Table S7. Ezetimibe registry: demographic and clinical features of patients without ezetimibe treatment

		Baseline (BL)	Follow-up (FU)	n¹	<i>P</i> value (BL vs. FU)
General	Sex, male/female	7/1	7/1	8/8	-
	Age, y	75.5± 10.9	76.9± 10.7	8/8	-
	BMI, kg/m ²	28.0± 4.5	27.9± 4.1	8/8	1.000
Medical History	CAD, n	5	5	8/8	1.000
	AVD, n	1	1	8/8	1.000
	DCM, n	1	1	8/8	1.000
	Hypertension, n	5	5	8/8	1.000
	Diabetes, n	3	3	8/8	1.000
	Hyperlipidemia, n	7	7	8/8	1.000
CC	Creatinin, µmol/L	1.02±0.38	1.07±0.37	8/8	0.100
	NT-proBNP, ng/L	381.0±174.5	540.8±458.5	5/5	1.000
	Potassium, mmol/L	3.94±1.22	4.41±0.41	8/8	0.620
	eGFR	75.4±24.9	69.5±23.2	8/8	0.070
Echocardiography	LAD, mm	42.0±4.1	42.5±2	8/8	1.000
	LVEDD, mm	52.0±11.1	49.4±7.7	8/8	0.602
	IVSd, mm	11.4±1.8	11.5±1.9	8/8	1.000
	LVPWd, mm	10.4±2.0	10.5±1.9	8/8	1.000
	LVEF, %	46.0±9.2	46.1±9.6	8/8	0.748
	E/A	0.47±0.45	1.37±0.60	3/3	0.214

	E/E'	9.4±3.1	10.1±3.2	7/7	0.284
Medication	ACE inhibitors, n	3	3	8/8	1.000
	ASS, n	2	2	8/8	1.000
	AT1 blockers, n	4	3	8/8	1.000
	β-Blockers, n	7	7	8/8	1.000
	Digitalis, n	1	1	8/8	1.000
	Dihydropyridines, n	1	1	8/8	1.000
	Diuretics, n	5	6	8/8	1.000
	DOAC, n	6	6	8/8	1.000
	LLD, n	6	6	8/8	1.000
	NEPi, n	0	0	8/8	1.000
	Nitrates, n	0	0	8/8	1.000
	Marcumar	1	1	8/8	1.000

ACE, angiotensin-converting enzyme; ASS, acetylsalicylic acid; AT, angiotensin receptor; AVD, aortic valve disease BMI, body mass index; CC, clinical chemistry; CAD, coronary artery disease; DCM, dilated cardiomyopathy; DOAC, direct oral anticoagulants; E/A, early to late diastolic transmitral flow velocity; E/E', early diastolic transmitral flow velocity to early diastolic mitral annular tissue velocity; eGFR, estimated glomerular filtration rate; IVSd, interventricular septum thickness at end-diastole; LAD, left atrial diameter; LLD, lipid-lowering drugs; LVEDD, left ventricular end-diastolic diameter; LVEF, left ventricular ejection fraction; LVPWd, left ventricular posterior wall thickness at end-diastole; NEPi, Neprilysin Inhibitor; NT-proBNP, N-terminal pro-B-type natriuretic peptide; n, number of patients; n¹, number of patients from whom data were available for each parameter out of the total cohort. Continuous data are expressed as mean ± SD. *P* values were calculated using Student *t* test and Fisher's exact test (Bonferroni-adjusted for multiple comparisons).

Supplemental Table S8. Ezetimibe registry: demographic and clinical features of patients who initiated ezetimibe during follow-up (FU)

		Baseline (BL)	Follow-up (FU)	n ¹	P (BL vs. FU)	P (BL vs. Ctrl. BL) ²
General	Sex, male/female	14/0	14/0	14/14	-	-
	Age, y	70.8±8.8	72.6±8.7	14/14	-	0.558
	BMI, kg/m ²	28.3±5.0	28.3±4.9	14/14	1.000	1.000
Medical History	CAD, n	12	12	14/14	1.000	0.618
	AVD, n	1	1	14/14	1.000	1.000
	DCM, n	1	1	14/14	1.000	1.000
	Hypertension, n	11	11	14/14	1.000	1.000
	Diabetes, n	1	2	14/14	1.000	0.234
	Hyperlipidemia, n	14	14	14/14	1.000	0.728
CC	Creatinin, µmol/L	1.09±0.26	1.10±0.30	13/13	1.000	1.000
	NT-proBNP, ng/L	786.0±1050.2	562.75±472.2	8/8	1.000	0.463
	Potassium, mmol/L	4.31±0.38	4.49±0.55	13/13	0.704	0.640
	eGFR	69.1±18.7	70.3±18.0	13/13	1.000	1.000
Echocardiography	LAD, mm	42.6±4.1	43.9±2.6	14/14	0.604	1.000
	LVEDD, mm	52.6±6.1	51.8±4.7	14/14	1.000	1.000
	IVSd, mm	12.6±1.7	12.6±1.8	14/14	1.000	0.234
	LVPWd, mm	10.6±1.1	10.2±0.9	14/14	0.702	0.280
	LVEF, %	44.4±10.3	43.1±9.2	14/14	1.000	1.000
	E/A	0.86±0.33	0.75±0.22	13/13	0.614	0.200

Impaired atrial mitochondrial calcium handling in patients with atrial fibrillation
Circulation Research

	E/E'	8.9±2.7	7.9±2.7	12/12	0.758	1.000
Medication	ACE inhibitors, n	6	6	14/14	1.000	1.000
	ASS, n	2	0	14/14	1.000	1.000
	AT1 blockers, n	4	2	14/14	1.000	0.772
	β-Blockers, n	11	11	14/14	1.000	1.000
	Digitalis, n	1	1	14/14	1.000	1.000
	Dihydropyridines, n	1	1	14/14	1.000	1.000
	Diuretics, n	10	10	14/14	1.000	0.610
	DOAC	11	12	14/14	1.000	1.000
	LLD, n	12	12	14/14	1.000	1.000
	NEPi, n	3	4	14/14	1.000	0.546
	Nitrates, n	0	0	14/14	1.000	-
	Marcumar, n	2	2	14/14	1.000	1.000

ACE, angiotensin-converting enzyme; ASS, Acetylsalicylic acid; AT, angiotensin receptor; AVD, aortic valve disease BMI, body mass index; CC, clinical chemistry; CAD, coronary artery disease; DCM, dilated cardiomyopathy; DOAC, direct oral anticoagulants; E/A, early to late diastolic transmitral flow velocity; E/E', early diastolic transmitral flow velocity to early diastolic mitral annular tissue velocity; eGFR, estimated glomerular filtration rate; IVSd, interventricular septum thickness at end-diastole; LAD, left atrial diameter; LLD, lipid-lowering drugs; LVEDD, left ventricular end-diastolic diameter; LVEF, left ventricular ejection fraction; LVPWd, left ventricular posterior wall thickness at end-diastole; NEPi, neprilysin inhibitor; NT-proBNP, N-terminal pro-B-type natriuretic peptide; n, number of patients; n¹, number of patients from whom data were available for each parameter out of the total cohort. ² Control patients without ezetimibe treatment are summarized in **Supplemental Table S7**. Continuous data are expressed as mean ± SD. *P* values were calculated using Student *t* test and Fisher's exact test (Bonferroni-adjusted for multiple comparisons.)

Supplemental Table S9. AF burden of patients before and after onset of ezetimibe therapy.

Control		Ezetimibe	
Baseline	Follow-up	Baseline	Follow-up
0.04604052	0.5461157	0.1	0.05
0.1	0.109	0.5	0.1
0.11200717	0.23293651	0.8	0.575
0.55932234	63.4920635	1	0.001
0.02038043	0.13	0.05	0.1
0.1	30.7212753	1	1
0.83709243	4.86053256	1	0.3333333
1	1.08333333	0.9	0.001
		0.1	0.001
		1	0.325
		1	1
		0.1	0.001
		0.5	0.3333333
		0.1333333	0.1

Supplemental Table S10. Antibodies used for immunofluorescent staining

Primary Antibody	Dilution	Company	Identifier
RyR2	1:500	Sigma	HPA020028
VDAC	1:200-500	NeuroMab	75-204
VDAC	1:200	LSBio	LS-C312926
β -tubulin	1:75	CST	#2146
TOM20	1:200	Proteintech	11802-1-AP
Secondary Antibody	Dilution	Company	Identifier
STAR 635P anti-rabbit IgG	1:1000	Abberior	ST635P-1002-500UG
STAR 580 anti-mouse IgG	1:1000	Abberior	ST580-1001-500UG

Supplemental Table S11. Antibodies used for immunoblots

Primary Antibody	Dilution	Company	Catalogue Number
PDH	1:1000	Abcam	ab110416
PDH-E1 pSer232	1:1000	Merck	AP1063
PDH-E1 pSer293	1:5000	Merck	ABS204
PDH-E1 pSer300	1:2000	Merck	ABS194
PDP1	1:5000	Sigma-Aldrich	HPA021152
PDK4	1:1000	Proteintech	12949-1-AP
mNCLX (SLC24A6)	1:500	Abcam	ab83551
VDAC1	1:2000	NeuroMab	75-204
VDAC2	1:2500	Abcam	ab37985
GRP75	1:2000	Sigma	HPA000898
TGM2	1:3000	Sigma	HPA029518
PTPIP51	1:2000	Sigma	HPA009975
VAPB	1:10000	Sigma	HPA013144
PDZD8	1:500	ThermoFischer	PA5-46771
MFN2	1:2000	Abcam	ab56889
FIS1	1:1000	Sigma-Aldrich	HPA017430
DRP1	1:1000	CST	#5391S
RyR2	1:1000	Thermo Fisher	MA3-916
RyR2 pSer2808	1:1000	Badrilla	A010-30
RyR2 pSer2814	1:500	Badrilla	A010-31
GAPDH	1:80000	Santa Cruz	sc-47724
Secondary Antibody	Dilution	Company	Catalogue Number
IRDye® 800CW Donkey anti-rabbit IgG	1:10000	Li-Cor	926-32213
IRDye® 800CW Donkey anti-goat IgG	1:10000	Li-Cor	926-32214
IRDye® 680RD Donkey anti-mouse IgG	1:10000	Li-Cor	926-68072
AzureSpectra 550 goat anti-mouse	1:2500	Azure Biosystems	512159

SUPPLEMENTAL STATISTICAL TABLE

Main Manuscript						
Figure Number	Normality	Statistical method	Post hoc correction	Comparison	Summary	Adjusted <i>P</i> value
1B	Yes	Two-way ANOVA	N/A	Ctrl (n=20 myocytes/11 patients) vs AF (n=21 myocytes/5 patients)	##	0.0071
	Yes	Multiple comparisons two-way ANOVA	Bonferroni	0.5 Hz Ctrl (n=20 myocytes/11 patients) vs 0.5 Hz AF (n=21 myocytes/5 patients)	**	0.0054
	Yes			3 Hz Ctrl (n=20 myocytes/11 patients) vs 3 Hz AF (n=21 myocytes/5 patients)	**	0.0030
	Yes			3 Hz + ISO Ctrl (n=20 myocytes/11 patients) vs 3 Hz + ISO AF (n=21 myocytes/5 patients)	ns	0.3674
1C	Yes	Student unpaired <i>t</i> test	N/A	Ctrl (n=13 myocytes/10 patients) vs AF (n=7 myocytes/4 patients)	ns	0.0865
1E	No	Mann-Whitney <i>U</i> test	N/A	Ctrl (n=13 myocytes/10 patients) vs AF (n=7 myocytes/4 patients)	*	0.0186
1F	Yes	Paired <i>t</i> test	N/A	3 Hz ss Ctrl vs 3 Hz peak Ctrl (n=13 myocytes/10 patients)	**	0.0030
	Yes	Paired <i>t</i> test	N/A	3 Hz ss AF vs 3 Hz peak AF (n=7 myocytes/4 patients)	ns	0.2244
1G	No	Mann-Whitney <i>U</i> test	N/A	Ctrl (n=13 myocytes/10 patients) vs AF (n=7 myocytes/4 patients)	*	0.0297
1H	No	Wilcoxon matched-pairs signed rank test	N/A	3 Hz + ISO ss Ctrl vs 3 Hz + ISO peak Ctrl (n=13 myocytes/10 patients)	***	0.0002
	Yes	Paired <i>t</i> test	N/A	3 Hz + ISO ss AF vs 3 Hz + ISO peak AF (n=7 myocytes/4 patients)	**	0.0027

1I	Yes	Welch <i>t</i> test	N/A	Ctrl (n=13 myocytes/10 patients) vs AF (n=7 myocytes/4 patients)	*	0.0495
2C(i)	Yes	Two-way ANOVA	N/A	Ctrl (n=17 myocytes/9 patients) vs AF (n=12 myocytes/8 patients)	ns	0.2962
	Yes	Multiple comparisons two-way ANOVA	Bonferroni	0.5 Hz Ctrl (n=17 myocytes/9 patients) vs 0.5 Hz AF (n=12 myocytes/8 patients)	ns	>0.9999
	Yes			3 Hz Ctrl (n=17 myocytes/9 patients) vs 3 Hz AF (n=12 myocytes/8 patients)	ns	0.9679
	Yes			3 Hz + ISO Ctrl (n=17 myocytes/9 patients) vs 3 Hz + ISO AF (n=12 myocytes/8 patients)	ns	0.9933
2C(ii)	Yes	Student unpaired <i>t</i> test	N/A	3 Hz Ctrl (n=17 myocytes/9 patients) vs 3 Hz AF (n=12 myocytes/8 patients)	ns	0.1987
	No	Mann-Whitney <i>U</i> test	N/A	3 Hz + ISO Ctrl (n=17 myocytes/9 patients) vs 3 Hz + ISO AF (n=12 myocytes/8 patients)	ns	0.0919
2E(i)	Yes	Two-way ANOVA	N/A	Ctrl (n=17 myocytes/9 patients) vs AF (n=12 myocytes/8 patients)	ns	0.0501
	Yes	Multiple comparisons two-way ANOVA	Bonferroni	0.5 Hz Ctrl (n=17 myocytes/9 patients) vs 0.5 Hz AF (n=12 myocytes/8 patients)	*	0.0391
	Yes			3 Hz Ctrl (n=17 myocytes/9 patients) vs 3 Hz AF (n=12 myocytes/8 patients)	*	0.0365
	Yes			3 Hz + ISO Ctrl (n=17 myocytes/9 patients) vs 3 Hz + ISO AF (n=12 myocytes/8 patients)	ns	0.0653
2E(ii)	No	Mann-Whitney <i>U</i> test	N/A	3 Hz Ctrl (n=17 myocytes/9 patients) vs 3 Hz AF (n=12 myocytes/8 patients)	*	0.0151
	No	Mann-Whitney <i>U</i> test	N/A	3 Hz + ISO Ctrl (n=17 myocytes/9 patients) vs 3 Hz + ISO AF (n=12 myocytes/8 patients)	ns	0.5047
2D(i)	Yes	Two-way ANOVA	N/A	Ctrl (n=17 myocytes/9 patients) vs AF (n=12 myocytes/8 patients)	#	0.0119

	Yes	Multiple comparisons two-way ANOVA	Bonferroni	0.5 Hz Ctrl (n=17 myocytes/9 patients) vs 0.5 Hz AF (n=12 myocytes/8 patients)	*	0.0490
	Yes			3 Hz Ctrl (n=17 myocytes/9 patients) vs 3 Hz AF (n=12 myocytes/8 patients)	**	0.0089
	Yes			3 Hz + ISO Ctrl (n=17 myocytes/9 patients) vs 3 Hz + ISO AF (n=12 myocytes/8 patients)	**	0.0051
2D(ii)	No	Mann-Whitney <i>U</i> test	N/A	3 Hz Ctrl (n=17 myocytes/9 patients) vs 3 Hz AF (n=12 myocytes/8 patients)	*	0.0270
	No	Mann-Whitney <i>U</i> test	N/A	3 Hz + ISO Ctrl (n=17 myocytes/9 patients) vs 3 Hz + ISO AF (n=12 myocytes/8 patients)	ns	0.9019
2F(i)	Yes	Two-way ANOVA	N/A	Ctrl (n=17 myocytes/9 patients) vs AF (n=12 myocytes/8 patients)	#	0.0266
	Yes	Multiple comparisons two-way ANOVA	Bonferroni	0.5 Hz Ctrl (n=17 myocytes/9 patients) vs 0.5 Hz AF (n=12 myocytes/8 patients)	ns	0.4089
	Yes			3 Hz Ctrl (n=17 myocytes/9 patients) vs 3 Hz AF (n=12 myocytes/8 patients)	ns	0.0736
	Yes			3 Hz + ISO Ctrl (n=17 myocytes/9 patients) vs 3 Hz + ISO AF (n=12 myocytes/8 patients)	*	0.0107
2F(ii)	No	Mann-Whitney <i>U</i> test	N/A	3 Hz Ctrl (n=17 myocytes/9 patients) vs 3 Hz AF (n=12 myocytes/8 patients)	ns	0.1273
	No	Mann-Whitney <i>U</i> test	N/A	3 Hz + ISO Ctrl (n=17 myocytes/9 patients) vs 3 Hz + ISO AF (n=12 myocytes/8 patients)	*	0.0235
2G	Yes	Two-way ANOVA	N/A	Ctrl (n=17 myocytes/9 patients) vs AF (n=12 myocytes/8 patients)	#	0.0476
	Yes	Multiple comparisons two-way ANOVA	Bonferroni	0.5 Hz Ctrl (n=17 myocytes/9 patients) vs 0.5 Hz AF (n=12 myocytes/8 patients)	ns	0.1651
	Yes			3 Hz Ctrl (n=17 myocytes/9 patients) vs 3 Hz AF (n=12 myocytes/8 patients)	*	0.0155

Impaired atrial mitochondrial calcium handling in patients with atrial fibrillation
Circulation Research

	Yes			3 Hz + ISO Ctrl (n=17 myocytes/9 patients) vs 3 Hz + ISO AF (n=12 myocytes/8 patients)	*	0.0147
3A	No	Multiple comparisons two-way ANOVA	N/A	Ctrl (n=35 patients) vs AF (n=11 patients)	ns	0.6499
3B	No	Multiple comparisons two-way ANOVA	N/A	Ctrl (n=35 patients) vs AF (n=11 patients)	ns	0.7948
3B	No	Mixed-effects analysis	Bonferroni	See Dataset_PTP Assay		
4C	Yes	Student unpaired <i>t</i> test	N/A	Ctrl (n=13 patients) vs AF (n=7 patients)	ns	0.6290
4D	Yes	Student unpaired <i>t</i> test	N/A	Ctrl (n=13 patients) vs AF (n=7 patients)	*	0.0308
4E	No	Mann-Whitney <i>U</i> test	N/A	Ctrl (n=13 patients) vs AF (n=7 patients)	****	5.16E-05
4H	N/A	Friedman's test	N/A	Ctrl (n=106 ROIs/9 patients) vs AF (n=106 ROIs/8 patients)	**	0.0018
4I	Yes	Student unpaired <i>t</i> test	N/A	Ctrl (n=9 patients) vs AF (n=8 patients)	*	0.0373
5B	No	Mann-Whitney <i>U</i> test	N/A	Ctrl (n=6 patients) vs AF (n=9 patients) Outliers: Ctrl (n=3), AF (n=1)	ns	0.1104
5C	Yes	Student unpaired <i>t</i> test	N/A	Ctrl (n=6 patients) vs AF (n=9 patients) Outliers: Ctrl (n=3), AF (n=1)	*	0.0605
5E	N/A	Chi-square test	N/A	Ctrl (n=97 ROIs/6 patients) vs AF (n=85 ROIs/9 patients) Outliers: Ctrl (n=27/3), AF (n=14/1)	****	8.78E-06
5G	No	Linear mixed- effects model	Šidák	Vehicle (n=78 cells/3 differentiations) vs Nocodazole (n=60 cells/3 differentiations)	****	2.76E-05

5H	No	Linear mixed-effects model	Šidák	Vehicle (n=87 cells/4 differentiations) vs Nocodazole (n=88 cells/4 differentiations)	*	0.0263
5J(i)	Yes			Nocodazole (n=95 cells/3 differentiations) vs DMSO (n=46 cells/3 differentiations)	****	<0.0001
	No			DMSO (n=46 cells/3 differentiations) vs Nocodazole+MitoTEMPO (n=65 cells/3 differentiations)	****	7.12E-06
	No			Nocodazole (n=95 cells/3 differentiations) vs. Nocodazole+MitoTEMPO (n=65 cells/3 differentiations)	****	2.43E-14
5J(ii)	No			Nocodazole (n=95 cells/3 differentiations) vs DMSO (n=46 cells/3 differentiations)	****	1.37E-05
	No			DMSO (n=46 cells/3 differentiations) vs Nocodazole+MitoTEMPO (n=65 cells/3 differentiations)	ns	0.9634
	No			Nocodazole (n=95 cells/3 differentiations) vs. Nocodazole+MitoTEMPO (n=65 cells/3 differentiations)	****	1.67E-05
5J(iii)	Yes			Nocodazole (n=95 cells/3 differentiations) vs DMSO (n=46 cells/3 differentiations)	**	0.0075
	No			DMSO (n=46 cells/3 differentiations) vs Nocodazole+MitoTEMPO (n=65 cells/3 differentiations)	ns	0.5226
	No			Nocodazole (n=95 cells/3 differentiations) vs. Nocodazole+MitoTEMPO (n=65 cells/3 differentiations)	ns	0.1534
5J(iv)	No			Nocodazole (n=95 cells/3 differentiations) vs DMSO (n=46 cells/3 differentiations)	*	0.0495
	No			DMSO (n=46 cells/3 differentiations) vs Nocodazole+MitoTEMPO (n=65 cells/3 differentiations)	ns	0.8019
	No	Linear mixed-effects model	Šidák	Nocodazole (n=95 cells/3 differentiations) vs. Nocodazole+MitoTEMPO (n=65 cells/3 differentiations)	ns	0.2398

5J(v)	No			Nocodazole (n=95 cells/3 differentiations) vs DMSO (n=46 cells/3 differentiations)	****	<0.0001
	No			DMSO (n=46 cells/3 differentiations) vs Nocodazole+MitoTEMPO (n=65 cells/3 differentiations)	*	1.22E-02
	No			Nocodazole (n=95 cells/3 differentiations) vs. Nocodazole+MitoTEMPO (n=65 cells/3 differentiations)	****	1.47E-12
5J(vi)	No			Nocodazole (n=95 cells/3 differentiations) vs DMSO (n=46 cells/3 differentiations)	****	1.34E-05
	No			DMSO (n=46 cells/3 differentiations) vs Nocodazole+MitoTEMPO (n=65 cells/3 differentiations)	ns	0.5161
	No			Nocodazole (n=95 cells/3 differentiations) vs. Nocodazole+MitoTEMPO (n=65 cells/3 differentiations)	****	6.31E-04
6A	No	Mann-Whitney <i>U</i> test	N/A	Vehicle (n=16 myocytes/7 patients) vs Ezetimibe (n=17 myocytes/7 patients)	*	0.0487
6C(i)	Yes	Student unpaired <i>t</i> test	N/A	Vehicle (n=31 myocytes/5 patients) vs Ezetimibe (n=20 myocytes/5 patients)	ns	0.4045
6C(ii)	No	Mann-Whitney <i>U</i> test	N/A	Vehicle (n=31 myocytes/5 patients) vs Ezetimibe (n=20 myocytes/5 patients)	**	0.0096
6C(iii)	No	Mann-Whitney <i>U</i> test	N/A	Vehicle (n=31 myocytes/5 patients) vs Ezetimibe (n=20 myocytes/5 patients)	**	0.0012
6E(i)	No	Mann-Whitney <i>U</i> test	N/A	Vehicle (n=31 myocytes/5 patients) vs Ezetimibe (n=20 myocytes/5 patients)	ns	0.1817
6E(ii)	No	Mann-Whitney <i>U</i> test	N/A	Vehicle (n=31 myocytes/5 patients) vs Ezetimibe (n=20 myocytes/5 patients)	ns	0.3119
6G(i)	No	Mann-Whitney <i>U</i> test	N/A	Vehicle (n=31 myocytes/5 patients) vs Ezetimibe (n=20 myocytes/5 patients)	*	0.0292
6G(ii)	No	Mann-Whitney <i>U</i> test	N/A	Vehicle (n=23 myocytes/5 patients) vs Ezetimibe (n=9 myocytes/4 patients)	ns	0.3207

7B(i)	No	Wilcoxon matched-pairs signed rank test	Bonferroni	BL vs Control (n=8 patients)	*	0.0156
7B(ii)	No	Wilcoxon matched-pairs signed rank test	Bonferroni	BL vs Ezetimibe (n=14 patients)	**	0.0020
7B (notshown)	No	Mann-Whitney <i>U</i> test	Bonferroni	Control (n=8 patients) vs Ezetimibe (n=14 patients)	ns	0.327
Supplementary Figures						
S1A	No	Mann-Whitney <i>U</i> test	N/A	Ctrl (n=50 patients) vs AF (n=20 patients)	*	0.0258
S1D(i)	Yes	Student unpaired <i>t</i> test	N/A	Ctrl (n=16 patients) vs AF (n=16 patients)	**	0.0093
S1D(ii)	Yes	Student unpaired <i>t</i> test	N/A	Ctrl (n=16 patients) vs AF (n=16 patients)	ns	0.5544
S1D(iii)	Yes	Welch <i>t</i> test	N/A	Ctrl (n=16 patients) vs AF (n=16 patients)	**	0.0086
S1D(iv)	No	Mann-Whitney <i>U</i> test	N/A	Ctrl (n=16 patients) vs AF (n=16 patients)	ns	0.2816
S1D(v)	No	Mann-Whitney <i>U</i> test	N/A	Ctrl (n=16 patients) vs AF (n=16 patients)	****	4.48E-05
S1D(vi)	No	Mann-Whitney <i>U</i> test	N/A	Ctrl (n=16 patients) vs AF (n=16 patients)	**	0.0020
S2A(i)	Yes	Two-way ANOVA	N/A	Ctrl (n=7 myocytes/3 patients) vs AF (n=4 myocytes/2 patients)	ns	0.0664
	Yes	Multiple comparisons	Bonferroni	3 Hz Ctrl (n=7 myocytes/3 patients) vs 3 Hz AF (n=4 myocytes/2 patients)	**	0.0026
	Yes	two-way ANOVA		6 Hz Ctrl (n=7 myocytes/3 patients) vs 6 Hz AF (n=4 myocytes/2 patients)	ns	0.0804

Impaired atrial mitochondrial calcium handling in patients with atrial fibrillation
Circulation Research

S2A(ii)	Yes	Two-way ANOVA	N/A	Ctrl (n=7 myocytes/3 patients) vs AF (n=4 myocytes/2 patients)	#	0.0367
	Yes	Multiple comparisons two-way ANOVA	Bonferroni	0.5 Hz Ctrl (n=7 myocytes/3 patients) vs 0.5 Hz AF (n=4 myocytes/2 patients)	*	0.0170
	Yes			3 Hz Ctrl (n=7 myocytes/3 patients) vs 3 Hz AF (n=4 myocytes/2 patients)	*	0.0135
	Yes			6 Hz Ctrl (n=7 myocytes/3 patients) vs 6 Hz AF (n=4 myocytes/2 patients)	ns	0.0936
S2B(i)	Yes	Two-way ANOVA	N/A	Ctrl (n=7 myocytes/3 patients) vs AF (n=7 myocytes/3 patients)	ns	0.1013
	Yes	Multiple comparisons two-way ANOVA	Bonferroni	3 Hz Ctrl (n=7 myocytes/3 patients) vs 3 Hz AF (n=7 myocytes/3 patients)	ns	0.1102
	Yes			6 Hz Ctrl (n=7 myocytes/3 patients) vs 6 Hz AF (n=7 myocytes/3 patients)	ns	0.1457
S2B(ii)	Yes	Two-way ANOVA	N/A	Ctrl (n=7 myocytes/3 patients) vs AF (n=7 myocytes/3 patients)	###	0.0066
	Yes	Multiple comparisons two-way ANOVA	Bonferroni	0.5 Hz Ctrl (n=7 myocytes/3 patients) vs 0.5 Hz AF (n=7 myocytes/3 patients)	**	0.0096
	Yes			3 Hz Ctrl (n=7 myocytes/3 patients) vs 3 Hz AF (n=7 myocytes/3 patients)	*	0.0312
	Yes			6 Hz Ctrl (n=7 myocytes/3 patients) vs 6 Hz AF (n=7 myocytes/3 patients)	**	0.0020
S3B(i)	No	Mann-Whitney <i>U</i> test	N/A	Ctrl (n=12 myocytes/3 pigs) vs AF (n=27 myocytes/3 pigs)	***	0.0004
S3B(ii) diastolic	No	Mann-Whitney <i>U</i> test	N/A	Ctrl (n=12 myocytes/3 pigs) vs AF (n=27 myocytes/3 pigs)	ns	0.3427
S3B(ii) systolic	No	Mann-Whitney <i>U</i> test	N/A	Ctrl (n=12 myocytes/3 pigs) vs AF (n=27 myocytes/3 pigs)	**	0.0058

Impaired atrial mitochondrial calcium handling in patients with atrial fibrillation
Circulation Research

S3B(iii)	No	Mann-Whitney <i>U</i> test	N/A	Ctrl (n=12 myocytes/3 pigs) vs AF (n=27 myocytes/3 pigs)	**	0.0022
S3B(iv)	No	Mann-Whitney <i>U</i> test	N/A	Ctrl (n=12 myocytes/3 pigs) vs AF (n=27 myocytes/3 pigs)	ns	0.6417
S3C(i)	No	Mann-Whitney <i>U</i> test	N/A	Ctrl (n=12 myocytes/3 pigs) vs AF (n=27 myocytes/3 pigs)	**	0.0013
S3C(ii) diastolic	No	Mann-Whitney <i>U</i> test	N/A	Ctrl (n=12 myocytes/3 pigs) vs AF (n=27 myocytes/3 pigs)	**	0.0079
S3C(ii) systolic	No	Mann-Whitney test	N/A	Ctrl (n=12 myocytes/3 pigs) vs AF (n=27 myocytes/3 pigs)	**	0.0058
S3C(iii)	No	Mann-Whitney <i>U</i> test	N/A	Ctrl (n=12 myocytes/3 pigs) vs AF (n=27 myocytes/3 pigs)	***	0.0009
S3C(iv)	No	Mann-Whitney <i>U</i> test	N/A	Ctrl (n=12 myocytes/3 pigs) vs AF (n=27 myocytes/3 pigs)	ns	0.0748
S3D(i)	Yes	Student unpaired <i>t</i> test	N/A	Ctrl (n=12 myocytes/3 pigs) vs AF (n=27 myocytes/3 pigs)	ns	0.9624
S3D(ii) diastolic	No	Mann-Whitney <i>U</i> test	N/A	Ctrl (n=12 myocytes/3 pigs) vs AF (n=27 myocytes/3 pigs)	*	0.0305
S3D(ii) systolic	No	Mann-Whitney <i>U</i> test	N/A	Ctrl (n=12 myocytes/3 pigs) vs AF (n=27 myocytes/3 pigs)	*	0.0219
S3D(iii)	No	Mann-Whitney <i>U</i> test	N/A	Ctrl (n=12 myocytes/3 pigs) vs AF (n=27 myocytes/3 pigs)	ns	0.3584
S3D(iv)	Yes	Welch <i>t</i> test	N/A	Ctrl (n=12 myocytes/3 pigs) vs AF (n=27 myocytes/3 pigs)	*	0.0423
S3E(ii)	No	Mann-Whitney <i>U</i> test	N/A	Ctrl (n=12 myocytes/3 pigs) vs AF (n=27 myocytes/3 pigs)	ns	>0.9999
S4A 0.5 Hz	No	Mann-Whitney <i>U</i> test	N/A	Ctrl (n=62 myocytes/5 patients) vs AF (n=34 myocytes/2 patients)	****	2.18E-09
S4A 3 Hz	No	Mann-Whitney <i>U</i> test	N/A	Ctrl (n=62 myocytes/5 patients) vs AF (n=34 myocytes/2 patients)	****	4.26E-09

Impaired atrial mitochondrial calcium handling in patients with atrial fibrillation
Circulation Research

S4B	No	Mann-Whitney <i>U</i> test	N/A	Ctrl (n=15) vs AF (n=16) 1 Ctrl patient did not show a band	ns	0.8304
S5B						
VDAC1	No	Mann-Whitney <i>U</i> test	N/A	Ctrl (n=16 patients) vs AF (n=16 patients)	ns	0.7448
VDAC2	No	Mann-Whitney <i>U</i> test	N/A	Ctrl (n=16 patients) vs AF (n=16 patients)	ns	0.5575
GRP75	No	Mann-Whitney <i>U</i> test	N/A	Ctrl (n=16 patients) vs AF (n=16 patients)	ns	0.6156
TGM2	No	Mann-Whitney <i>U</i> test	N/A	Ctrl (n=16 patients) vs AF (n=16 patients)	ns	0.5896
PTPIP51	No	Mann-Whitney <i>U</i> test	N/A	Ctrl (n=16 patients) vs AF (n=16 patients)	ns	0.3045
VAPB	No	Mann-Whitney <i>U</i> test	N/A	Ctrl (n=16 patients) vs AF (n=16 patients)	ns	0.2542
DPDZD8	Yes	Student unpaired <i>t</i> test	N/A	Ctrl (n=16 patients) vs AF (n=16 patients)	ns	0.0598
MFN2	No	Mann-Whitney <i>U</i> test	N/A	Ctrl (n=16 patients) vs AF (n=16 patients)	ns	0.5896
FIS1	No	Mann-Whitney <i>U</i> test	N/A	Ctrl (n=16 patients) vs AF (n=16 patients)	ns	0.1188
DRP1	Yes	Welch <i>t</i> test	N/A	Ctrl (n=16 patients) vs AF (n=16 patients)	ns	0.9935
S6B(i)	No	Mann-Whitney <i>U</i> test	N/A	DMSO (n=117 cells/3 differentiations) vs MitoTEMPO (n=85 cells/3 differentiations)	ns	0.3163
S6B(ii)	No	Mann-Whitney <i>U</i> test	N/A	DMSO (n=117 cells/3 differentiations) vs MitoTEMPO (n=85 cells/3 differentiations)	ns	0.2531
S6B(iii)	Yes	Student unpaired <i>t</i> test	N/A	DMSO (n=117 cells/3 differentiations) vs MitoTEMPO (n=85 cells/3 differentiations)	ns	0.3554
S6B(iv)	Yes	Student unpaired <i>t</i> test	N/A	DMSO (n=117 cells/3 differentiations) vs MitoTEMPO (n=85 cells/3 differentiations)	ns	0.4338

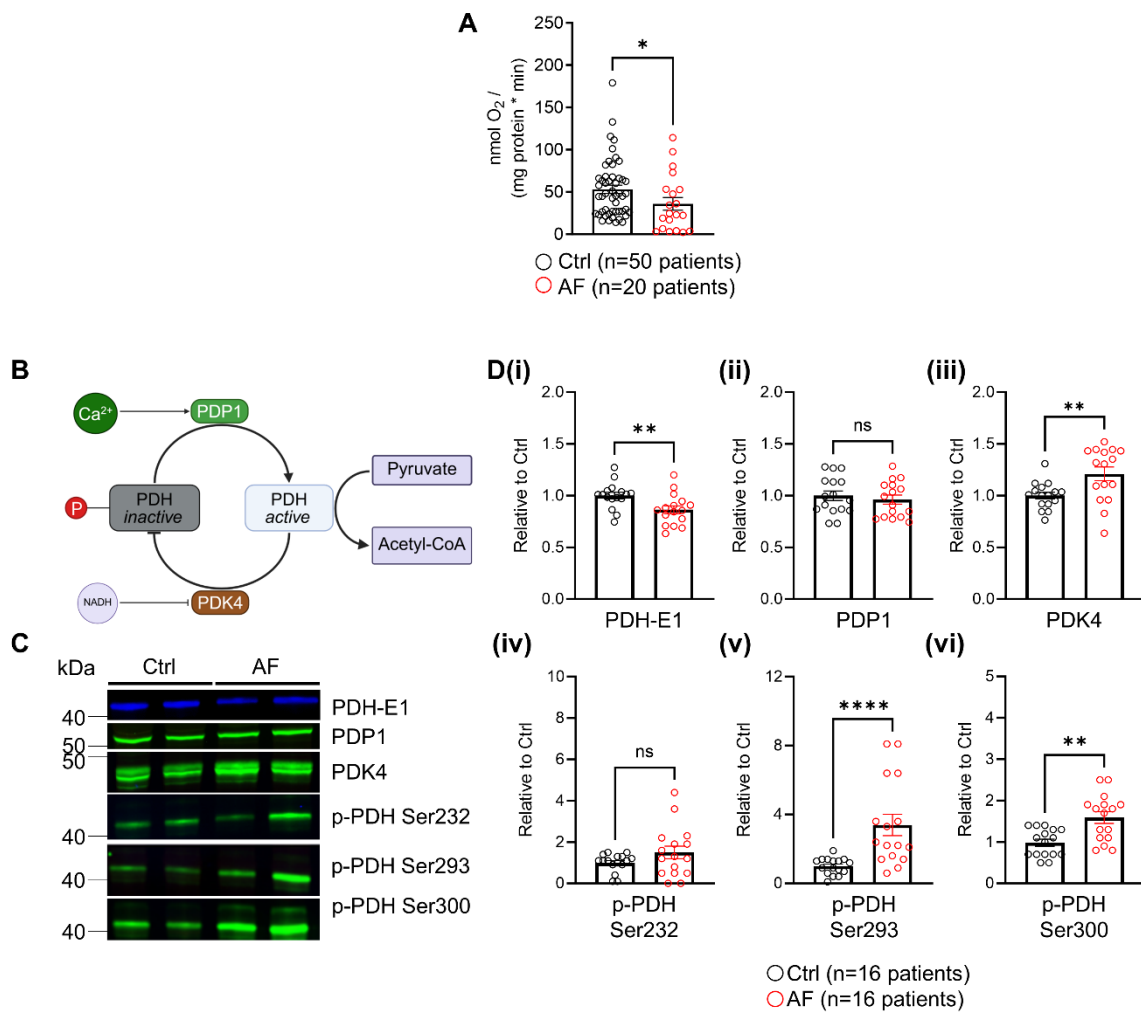
S6B(v)	No	Mann-Whitney <i>U</i> test	N/A	DMSO (n=117 cells/3 differentiations) vs MitoTEMPO (n=85 cells/3 differentiations)	ns	0.9593
S6B(vi)	No	Mann-Whitney <i>U</i> test	N/A	DMSO (n=117 cells/3 differentiations) vs MitoTEMPO (n=85 cells/3 differentiations)	ns	0.7188
S7B	Yes	Linear mixed- effects model	Šidák	Nocodazole (n=60 cells/3 differentiations) vs Nocodazole+Ezetimibe (n=40 cells/2 differentiations)	ns	0.1380
S7C	No			Nocodazole (n=84 cells/4 differentiations) vs Nocodazole+Ezetimibe (n=79 cells/4 differentiations)	ns	0.0754
S7E(i)	No			Nocodazole (n=56 cells/4 differentiations) vs Nocodazole+Ezetimibe (n=56 cells /4 differentiations)	****	1.21E-04
S7E(i)	No			Nocodazole (n=56 cells/4 differentiations) vs Nocodazole+Ezetimibe (n=56 cells /4 differentiations)	ns	0.4943
S7E(i)	Yes			Nocodazole (n=56 cells/4 differentiations) vs Nocodazole+Ezetimibe (n=56 cells /4 differentiations)	****	6.85E-05
S7E(i)	No			Nocodazole (n=56 cells/4 differentiations) vs Nocodazole+Ezetimibe (n=56 cells /4 differentiations)	****	9.65E-07
S7E(i)	No			Nocodazole (n=56 cells/4 differentiations) vs Nocodazole+Ezetimibe (n=56 cells /4 differentiations)	**	1.21E-03
S7E(i)	No			Nocodazole (n=56 cells/4 differentiations) vs Nocodazole+Ezetimibe (n=56 cells /4 differentiations)	****	9.71E-05
S8A	No	Mann-Whitney <i>U</i> test	N/A	Vehicle (n=31 myocytes/5 patients) vs Ezetimibe (n=20 myocytes/5 patients)	ns	0.5596
S9C	No	Wilcoxon matched-pairs signed rank test	N/A	Vehicle vs Ezetimibe (n=9 pigs)	ns	0.5703
S10A(ii)	No	Mann-Whitney <i>U</i> test	N/A	Vehicle (n=7 runs/4 differentiations) vs Ezetimibe (n=7 runs/4 differentiations)	ns	0.7104

S10A(iii)	Yes	Student unpaired <i>t</i> test	N/A	Vehicle (n=7 runs/4 differentiations) vs Ezetimibe (n=7 runs/4 differentiations)	ns	0.2675
S10B(ii)	Yes	Student unpaired <i>t</i> test	N/A	Vehicle (n=7 runs/4 differentiations) vs Ezetimibe (n=7 runs/4 differentiations)	ns	0.4655
S10B(iii)	No	Mann-Whitney <i>U</i> test	N/A	Vehicle (n=7 runs/4 differentiations) vs Ezetimibe (n=7 runs/4 differentiations)	ns	>0.9999
S11	No	Two-way ANOVA	NA	Ctrl (n=15 patients) vs (AF=30 patients)	ns	0.7139
	No	Multiple comparisons two-way ANOVA	Bonferroni	Row 2 Ctrl (n=15) vs (AF=30)	ns	0.3768
				Row 3 Ctrl (n=15) vs (AF=30)	ns	0.8564
				Row 4 Ctrl (n=15) vs (AF=30)	ns	0.3353
				Row 5 Ctrl (n=15) vs (AF=30)	ns	0.8214
				Row 6 Ctrl (n=15) vs (AF=30)	ns	0.9091
				Row 7 Ctrl (n=15) vs (AF=30)	ns	0.7434
				Row 8 Ctrl (n=15) vs (AF=30)	ns	0.9819
				Row 9 Ctrl (n=15) vs (AF=30)	ns	0.6926
				Row 10 Ctrl (n=15) vs (AF=30)	ns	0.6358
				Row 11 Ctrl (n=15) vs (AF=30)	ns	0.911
				Row 12 Ctrl (n=15) vs (AF=30)	ns	0.7144
				Row 13 Ctrl (n=15) vs (AF=30)	ns	0.7783
				Row 14 Ctrl (n=15) vs (AF=30)	ns	0.9517
				Row 15 Ctrl (n=15) vs (AF=30)	ns	0.5316
				Row 16 Ctrl (n=15) vs (AF=30)	ns	0.681
				Row 17 Ctrl (n=15) vs (AF=30)	ns	0.7109
				Row 18 Ctrl (n=15) vs (AF=30)	ns	0.4837
				Row 19 Ctrl (n=15) vs (AF=30)	ns	0.5444
				Row 20 Ctrl (n=15) vs (AF=30)	ns	0.4468
				Row 21 Ctrl (n=15) vs (AF=30)	ns	0.5823

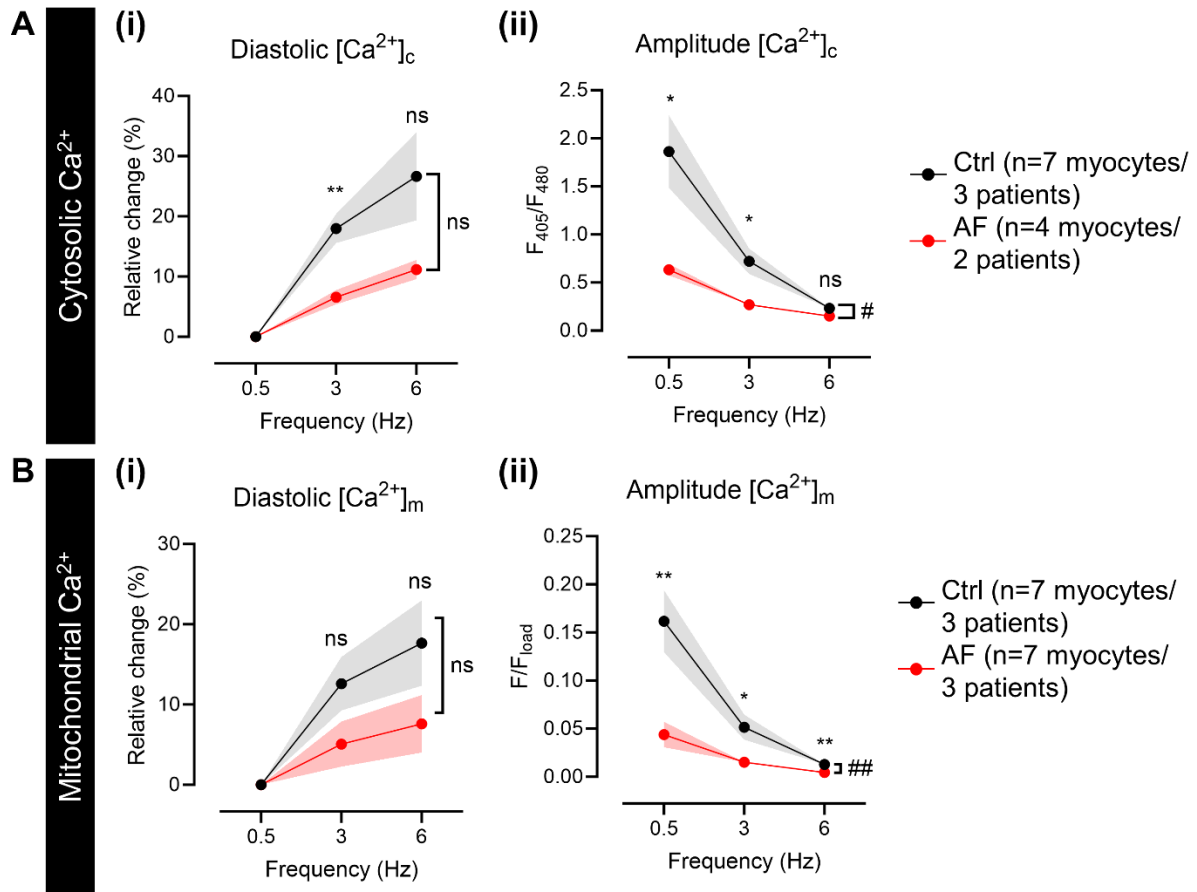
Impaired atrial mitochondrial calcium handling in patients with atrial fibrillation
Circulation Research

				Row 22 Ctrl (n=15) vs (AF=30)	ns	0.5911
				Row 23 Ctrl (n=15) vs (AF=30)	ns	0.3827
				Row 24 Ctrl (n=15) vs (AF=30)	ns	0.3497
				Row 25 Ctrl (n=15) vs (AF=30)	ns	0.3361
				Row 26 Ctrl (n=15) vs (AF=30)	ns	0.2601
				Row 27 Ctrl (n=15) vs (AF=30)	ns	0.4593
				Row 28 Ctrl (n=15) vs (AF=30)	ns	0.4155
				Row 29 Ctrl (n=15) vs (AF=30)	ns	0.1871
				Row 30 Ctrl (n=15) vs (AF=30)	ns	0.9787
				Row 31 Ctrl (n=15) vs (AF=30)	ns	0.9872
				Row 32 Ctrl (n=15) vs (AF=30)	ns	0.9751
				Row 33 Ctrl (n=15) vs (AF=30)	ns	0.9737
				Row 34 Ctrl (n=15) vs (AF=30)	ns	0.9726
				Row 35 Ctrl (n=15) vs (AF=30)	ns	0.9614
				Row 36 Ctrl (n=15) vs (AF=30)	ns	0.9776

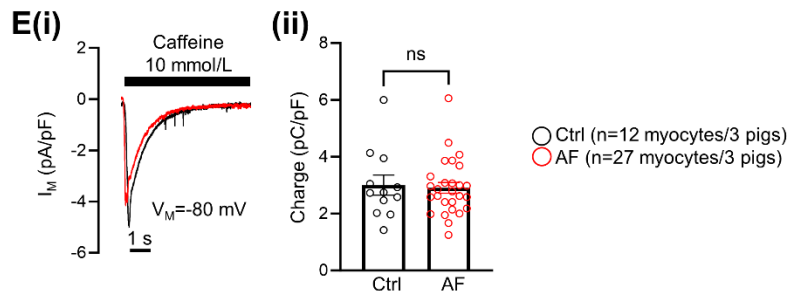
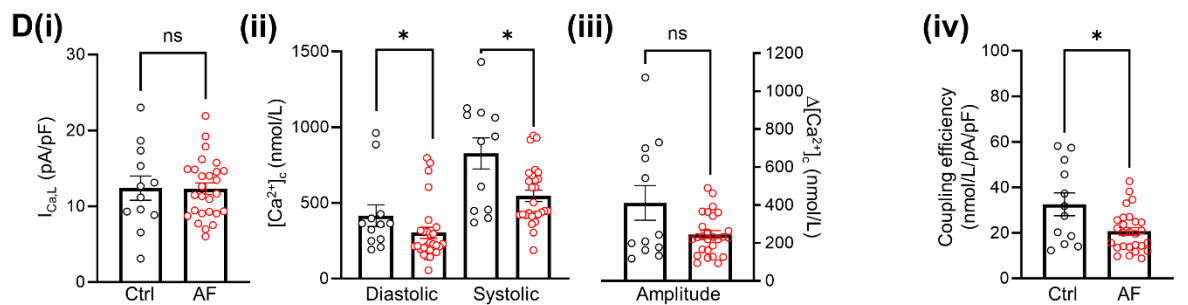
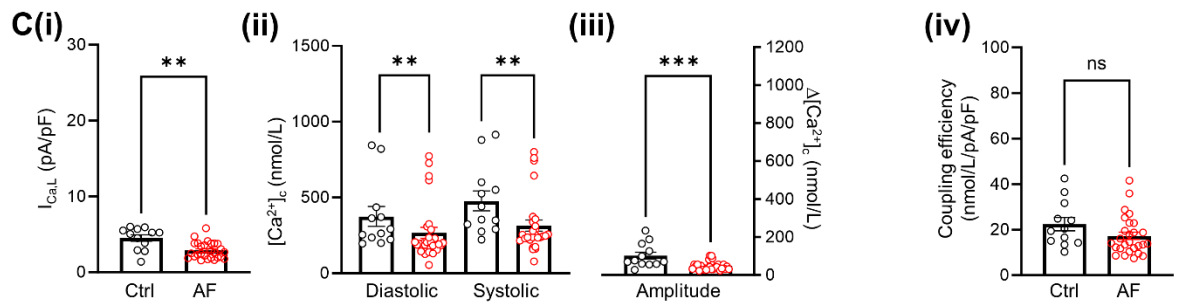
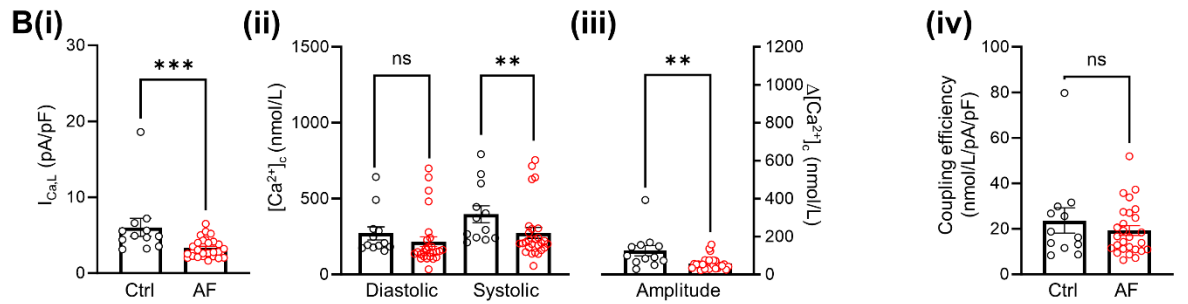
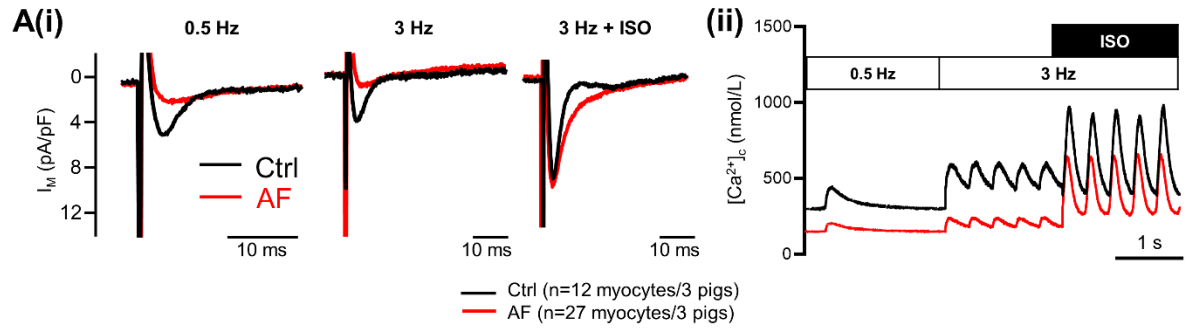
Supplemental Figures



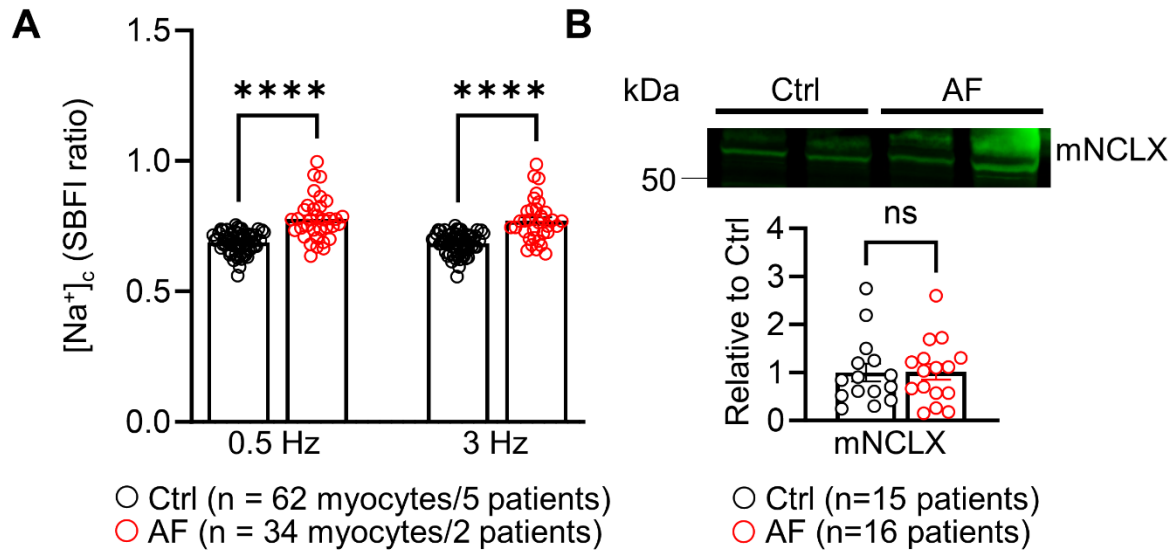
Supplemental Figure S1. Impaired oxidation of NADH and FADH₂ contributes to their accumulation which limits the activity of the tricarboxylic acid cycle. **A**, Mean \pm SEM oxygen consumption at state 3 respiration (1 mM ADP) of mitochondria from Ctrl and AF patients. *P* value was determined by Mann-Whitney *U* test. **P*<0.05. **B**, Simplified diagram of pyruvate dehydrogenase (PDH) showing the activation and inactivation by PDH phosphatase 1 (PDP1) and PDH kinase 4 (PDK4), respectively. PDP1 is the known Ca²⁺ sensitive enzyme that activates PDH. Striated muscle expresses predominantly PDK4 and is most sensitive to NADH. **C**, Representative immunoblots of the PDH-E1 subunit, PDP1, PDK4 and PDH-E1 phosphosites, Ser232, Ser293, and Ser300 and **D**, the corresponding mean \pm SEM of their densitometric analyses. All proteins were normalized to the total protein lanes (see Unedited Immunoblots) and normalized to Ctrl samples. Representative traces were selected to reflect the reported means. *P* values were determined by Student unpaired *t* test (**Di-ii**), Welch *t* test (**Diii**), or Mann-Whitney *U* test (**Div-vi**). ***P*<0.01, *****P*<0.0001. ADP indicates adenosine diphosphate; and ns indicates not significant.



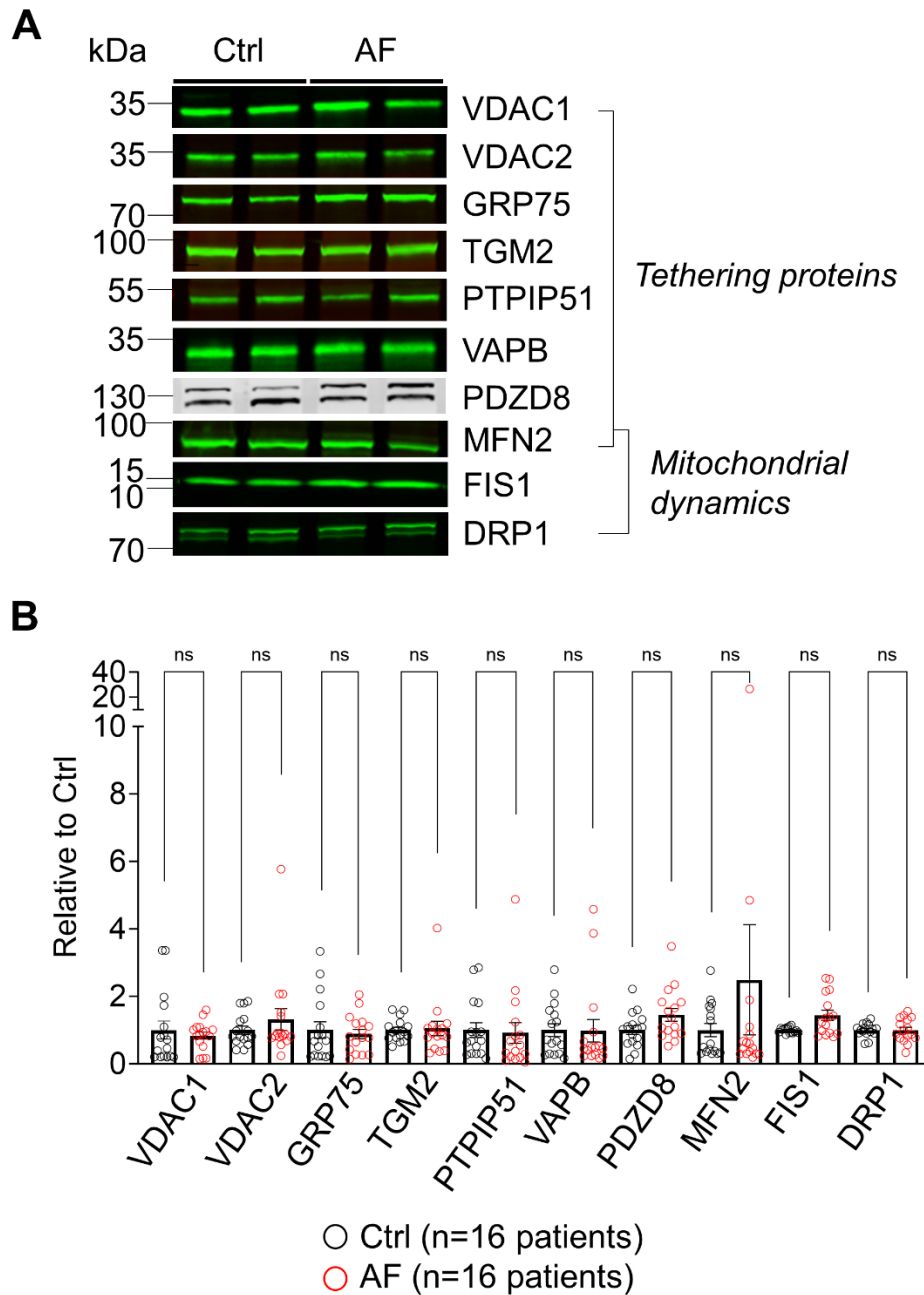
Supplemental Figure S2. Cytosolic and mitochondrial Ca^{2+} levels at increased stimulation frequencies in the absence of beta-adrenergic stimulation. **A**, Relative change in diastolic Ca^{2+} levels (**Ai**) and amplitude of Ca^{2+} transients (**Aii**) in the cytosol ($[\text{Ca}^{2+}]_c$). **B**, Relative change in diastolic Ca^{2+} levels (**Bi**) and amplitude of Ca^{2+} transients (**Bii**) in the mitochondria ($[\text{Ca}^{2+}]_m$). P values were determined by two-way ANOVA followed by Bonferonni post hoc correction. # $P < 0.05$, ## $P < 0.01$ with two-way ANOVA. * $P < 0.05$, ** $P < 0.01$ with Bonferonni post hoc correction. ns indicates not significant.



Supplemental Figure S3. Coupling efficiency between $I_{Ca,L}$ and cytosolic Ca^{2+} transients in a porcine AF model under increased workload. **A**, Representative traces of (i) L-type calcium current ($I_{Ca,L}$) and (ii) triggered Ca^{2+} transients at 0.5 Hz, 3 Hz, and 3 Hz with isoproterenol (ISO, 100 nmol/L) stimulation in atrial myocytes from control (Ctrl) and atrial fibrillation (AF). **B-D**, Mean \pm SEM (i) peak $I_{Ca,L}$, (ii) diastolic and systolic cytosolic Ca^{2+} concentration ($[Ca^{2+}]_c$), (iii) amplitude ($\Delta[Ca^{2+}]_c$), and (iv) coupling efficiency (defined as the ratio of Ca^{2+} release $[\Delta[Ca^{2+}]_c]$ to Ca^{2+} influx $[I_{Ca,L}]$) under baseline conditions (0.5 Hz, **B**), increased pacing frequency (3 Hz, **C**), and 3 Hz with ISO stimulation (3 Hz + ISO, **D**). **E**, Ca^{2+} load after 3 Hz + ISO. **(E)** Representative recordings of (i) caffeine-induced transient inward currents (I_{NCX}) in Ctrl and AF cardiac myocytes. (ii) Mean \pm SEM integrated I_{NCX} (charge accumulation) as a surrogate for Ca^{2+} content. Representative traces were selected to reflect the reported means. *P* values were determined by Mann-Whitney *U* test (**B**, **C**, **Dii-iii**, and **E**), Student unpaired *t* test (**Di**), or Welch *t* test (**Div**). **P*<0.05, ***P*<0.01, and ****P*<0.001 for unpaired comparisons. ns indicates not significant.

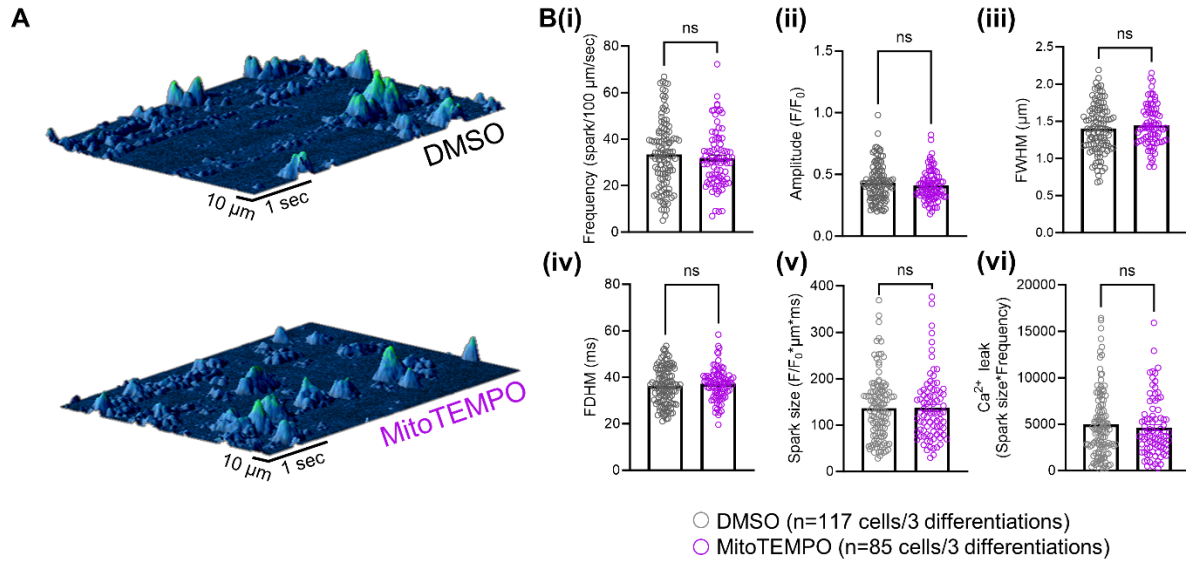


Supplemental Figure S4. Na^+ homeostasis in atrial myocytes from control (Ctrl) and atrial fibrillation (AF) patients. **A**, Mean \pm SEM intracellular Na^+ concentration quantified as SBFI ratio in atrial myocytes during steady state field stimulation at 0.5 and 3 Hz. **B**, Immunoblots (top) and mean \pm SEM (bottom) of mitochondrial Na^+ - Ca^{2+} exchanger (mNCLX) expression in atrial samples from Ctrl and AF patients, normalized to the total protein lanes (see Unedited Immunoblots) and normalized to Ctrl samples. *P* values were determined by Mann-Whitney *U* test. *****P* < 0.0001 for unpaired comparisons. kDa indicates kilodalton; and ns indicates not significant.

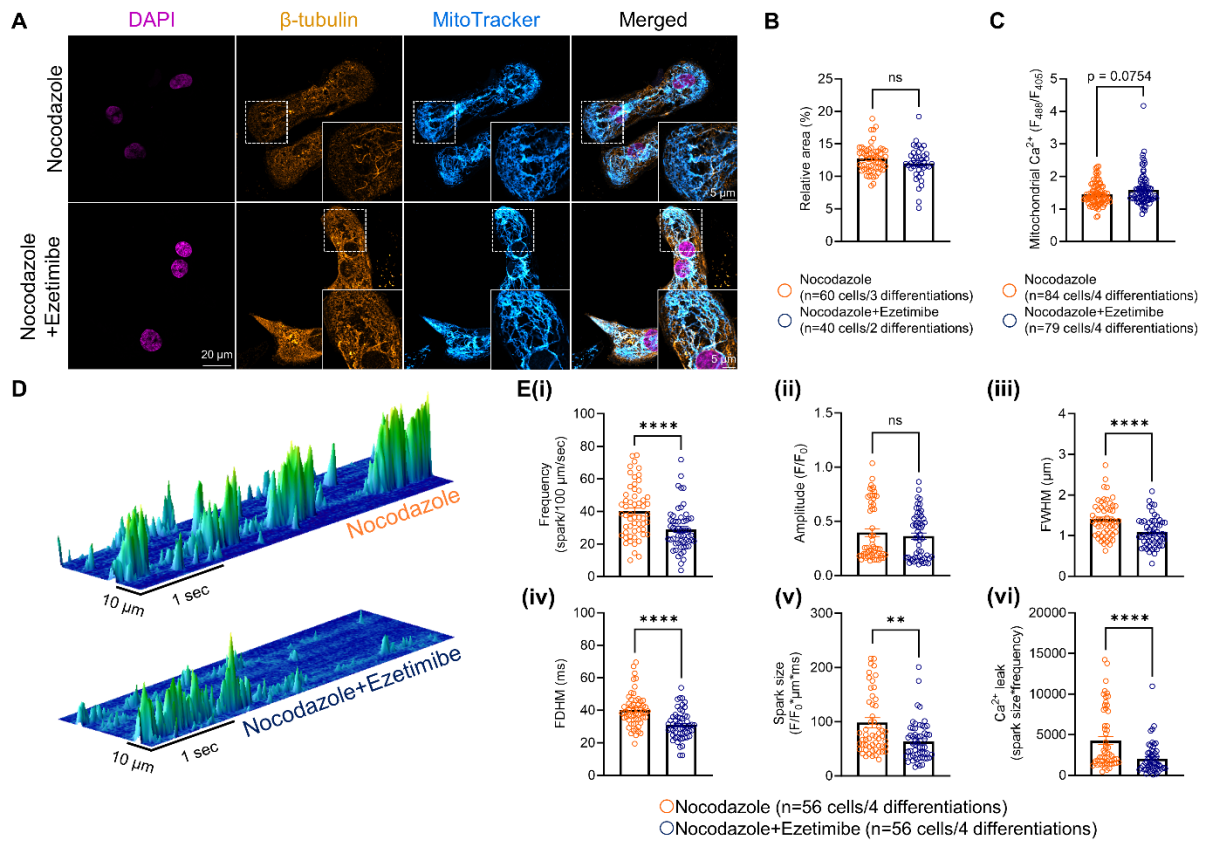


Supplemental Figure S5. Expression of SR-mitochondria tethering and mitochondrial dynamics proteins previously implicated in mitochondrial Ca^{2+} handling is unchanged.

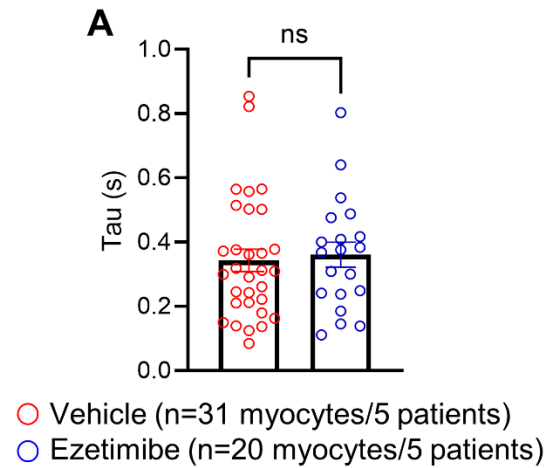
A, Representative immunoblots of key proteins involved in SR-mitochondria tethering and mitochondrial dynamics. **B**, Mean \pm SEM quantification of protein expression levels normalized to the total protein lanes (see Unedited Immunoblots) and then normalized to Ctrl samples. VDAC1/2 = Voltage-Dependent Anion Channel 1/2; GRP75 = Glucose-Regulated Protein 75; TGM2 = Transglutaminase 2; PTPIP51 = Protein Tyrosine Phosphatase-Interacting Protein 51; VAPB = Vesicle-Associated Membrane Protein-Associated Protein B; PDZD8 = PDZ Domain-Containing Protein 8; MFN2 = Mitofusin 2; FIS1 = Mitochondrial Fission 1 Protein; DRP1 = Dynamin-Related Protein 1. Representative images were selected to reflect the reported means. *P* values were determined by Mann-Whitney *U* test (VDAC1/2, GRP75, TGM2, PTPIP51, VAPB, MFN2, FIS1), Student unpaired *t* test (PDZD8), or Welch *t* test (DRP1). kDa indicates kilodalton; and ns indicates not significant.



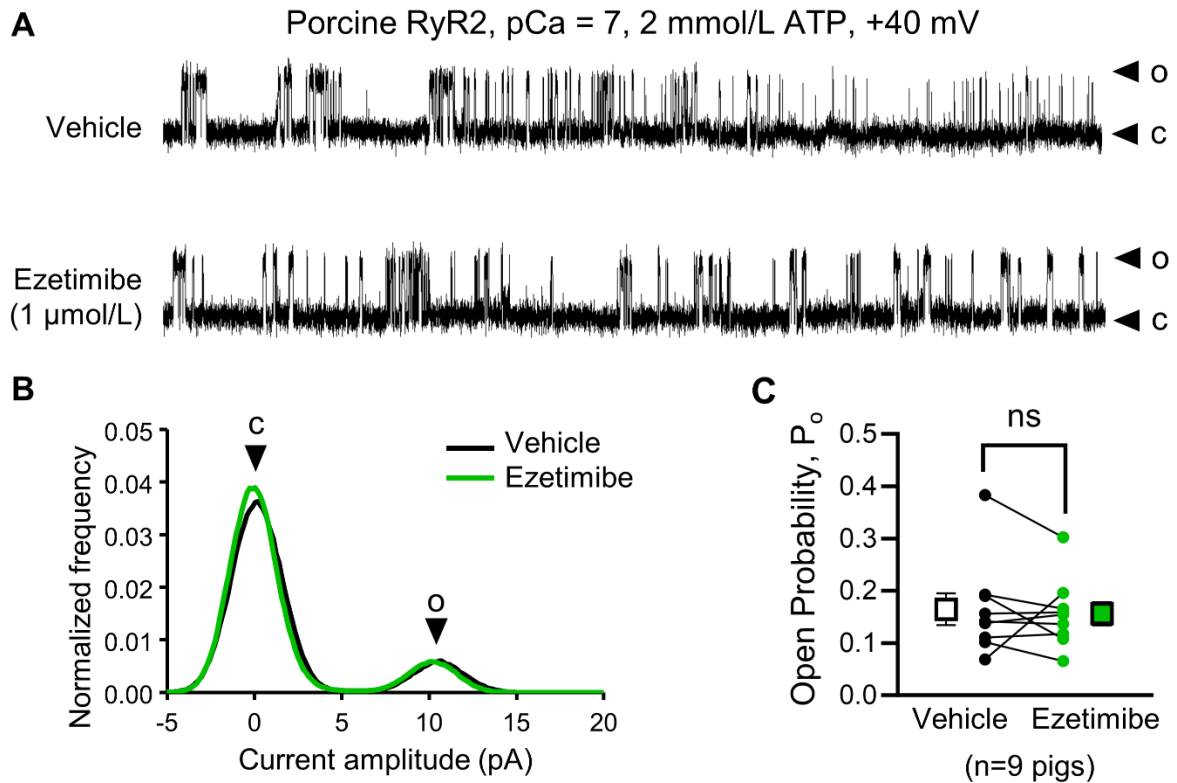
Supplemental Figure S6. MitoTEMPO has no effect on Ca^{2+} sparks in control atrial hiPSC-CMs. **A**, 3D line scans showing Ca^{2+} sparks. **B**, Mean \pm SEM of **(i)** Ca^{2+} spark frequency, **(ii)** amplitude, **(iii)** full-width half maximum (FWHM), **(iv)** full-duration half maximum (FDHM), **(v)** spark size, and **(vi)** Ca^{2+} leak. Representative images were selected to reflect the reported means. *P* values were determined by Mann-Whitney *U* test (**Bi-ii** and **Bv-vi**) or Student unpaired *t* test (**Biii-iv**). ns indicates not significant.



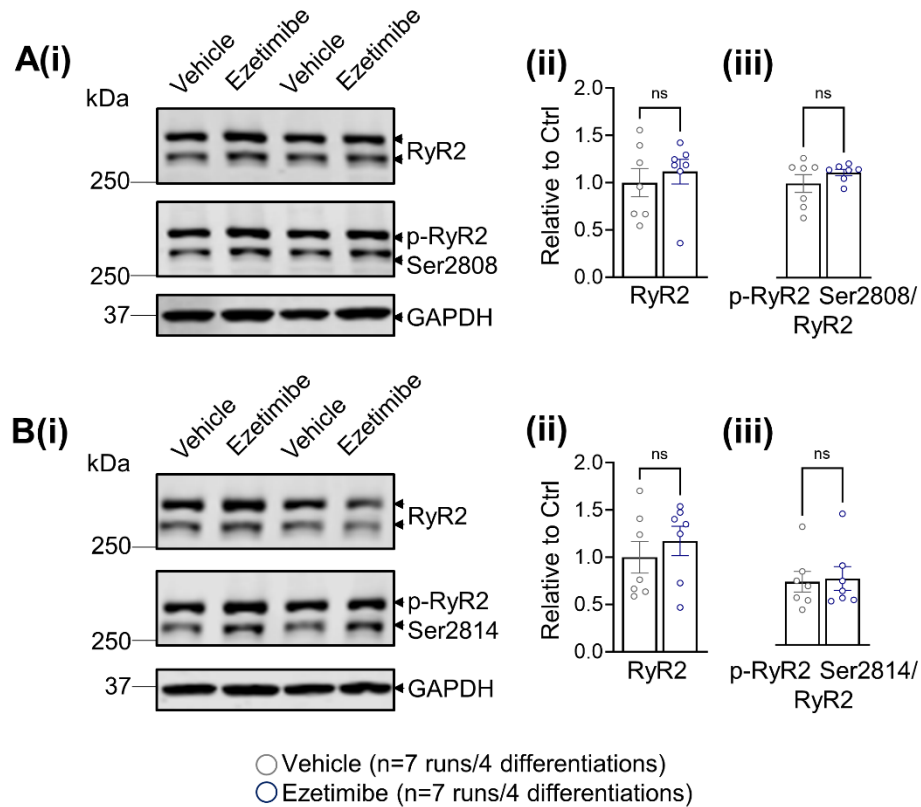
Supplemental Figure 7. Ezetimibe increases mitochondrial Ca^{2+} levels and rescues against Ca^{2+} sparks in hiPSC-CMs. **A**, Representative confocal images nocodazole-treated hiPSC-AMs with and without ezetimibe (1 μ mol/L, 1 h) showing nuclei (magenta), β -tubulin (orange) and MitoTracker (cyan). **B**, Mean \pm SEM of relative area occupied by mitochondria analyzed by MiNA plugin on Fiji. **C**, Mitochondrial Ca^{2+} level in hiPSC-CMs transfected with mito Pericam GFP. Ezetimibe improves calcium spark properties in hiPSC-AMs treated with nocodazole. **D**, 3D line scans and **E**, mean \pm SEM of (i) Ca^{2+} spark frequency, (ii) amplitude, (iii) full-width half maximum (FWHM), (iv) full-duration half maximum (FDHM), (v) spark size, and (vi) Ca^{2+} leak. Representative images were selected to reflect the reported means. P values were determined by a linear mixed-effects model with Šidák multiple comparisons post hoc test. ** $P < 0.01$ and **** $P < 0.0001$ for all comparisons. ns indicates not significant.



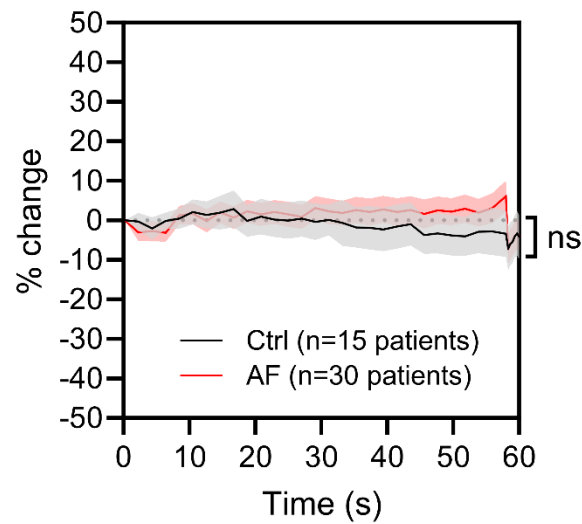
Supplemental Figure 8. Ezetimibe has no effect on cytosolic Ca^{2+} transient decay. A, Mean \pm SEM time constant (τ) of decay of Ca^{2+} transients stimulated at 0.5 Hz with and without 1 $\mu\text{mol/L}$ ezetimibe. P value was determined by Mann-Whitney U test. ns indicates not significant.



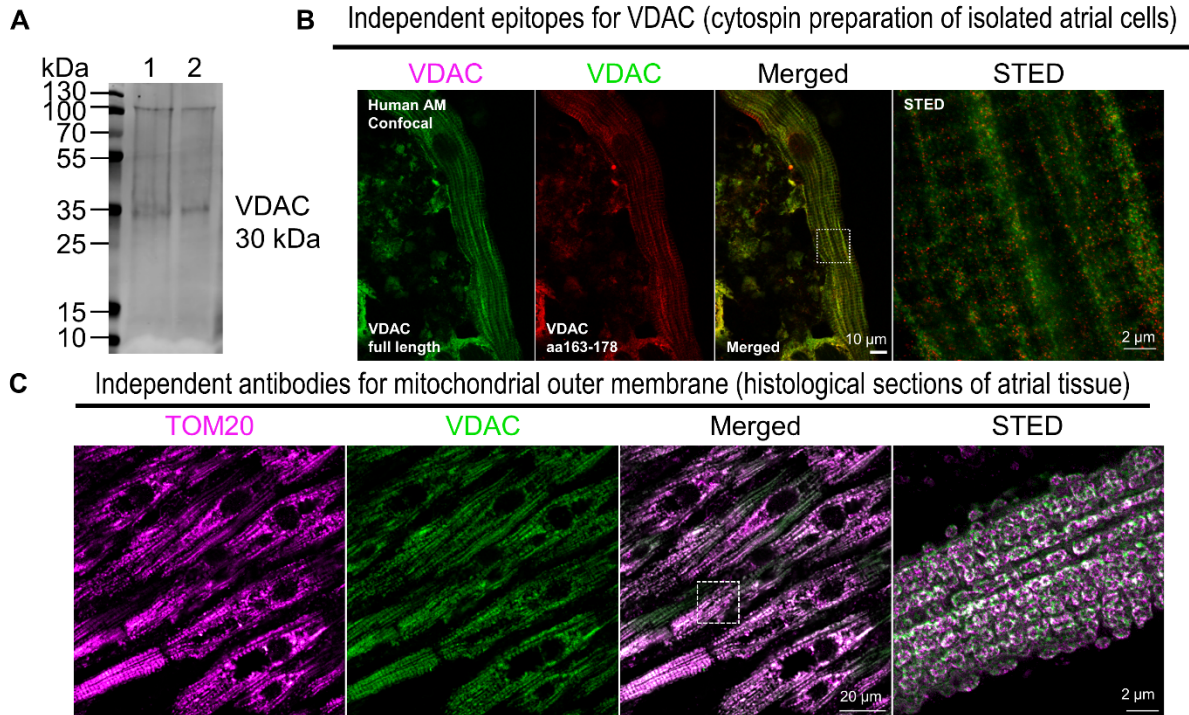
Supplemental Figure S9. Ezetimibe effects on RyR2 single-channel recordings. **A**, Single-channel tracings were obtained using planar lipid-bilayer recordings of RyR2 channels from pig ventricular cardiac myocytes in the absence (vehicle) and presence of ezetimibe (1 μ mol/L). Channel openings (o) are shown as upward deflections from the closed (c) level. **B**, Representative amplitude histogram indicating amplitudes of open (o) and closed (c) levels. **C**, Mean \pm SEM open probability (P_o) of RyR2 in absence and presence of ezetimibe (1 μ mol/L). P value was determined by Wilcoxon matched-pairs signed rank test. ns indicates not significant.



Supplemental Figure S10: Protein expression and phosphorylation status of RyR2 in atrial human induced pluripotent stem cell-derived cardiac myocyte (hiPSC-CM) treated with ezetimibe. **A**, Immunoblots (i) and quantification of the protein expression of ryanodine receptor 2 (ii, RyR2) and its phosphorylation at Serine 2808 (iii, pS2808-RyR2) in vehicle (DMSO)- and ezetimibe-treated (1 μ mol/L, 1 h) atrial hiPSC-CM. **B**, Immunoblots (i) and quantification of the protein expression RyR2 (ii) and its phosphorylation at serine 2814 (iii) in vehicle- and ezetimibe-treated hiPSC-CM. RyR2 was normalized to GAPDH. pS2808-RyR2 and pS2814-RyR2 were normalized to RyR2. Representative images were selected to reflect the reported means. *P* value was determined by Mann-Whitney *U* test (**Aii** and **Biii**) or Student *t* test (**Aiii** and **Bii**). kDa indicates kilodalton; and ns indicates not significant.



Supplemental Figure S11. Percentage change of peak L-type Ca^{2+} current during 0.5 Hz stimulation. *P* values were determined by two-way ANOVA followed by Bonferonni post hoc correction (detailed in Supplemental Statistical Table). ns indicates not significant.



Supplemental Figure S12. Validation of VDAC antibody used for STED imaging. **A**, Immunoblot of VDAC antibody showing a specific band at around 30 kDa. **B**, Confocal and STED images of VDAC with distinct epitopes. VDAC from NeuroMab used for our STED imaging was raised against a full-length human VDAC-GST fusion protein. Although the exact binding epitope is proprietary, specificity was independently confirmed with a second rabbit polyclonal antibody that binds on a known epitope of VDAC (aa 163–178), and yielded indistinguishable mitochondrial outer membrane staining patterns on cytospin preparations of isolated human atrial myocytes. **C**, A second outer membrane protein, TOM20, was used on histological sections of atrial tissues and also exhibited a similar staining pattern as VDAC from NeuroMab that was used for the study. aa indicates amino acid; and kDa indicates kilodalton.

Major Resources Table

In order to allow validation and replication of experiments, all essential research materials listed in the Methods should be included in the Major Resources Table below. Authors are encouraged to use public repositories for protocols, data, code, and other materials and provide persistent identifiers and/or links to repositories when available. Authors may add or delete rows as needed.

Animals (in vivo studies)

Species	Vendor or Source	Background Strain	Sex	Persistent ID / URL
<i>Sus scrofa domesticus</i>	Bräunling (Nussloch, Germany)	Landrace	M	N/A

Antibodies

Target antigen	Vendor or Source	Catalog #	Working concentration	Persistent ID / URL
RyR2	Sigma	HPA020028	1:500	RRID:AB_1856528
VDAC	NeuroMab	75-204	1:200-500	RRID:AB_2214807
VDAC	LSBio	LS-C312926	1:200	N/A
β -tubulin	CST	#2146	1:75	RRID:AB_2210545
TOM20	Proteintech	11802-1-AP	1:200	RRID:AB_2207530
PDH	Abcam	ab110416	1:1000	N/A
PDH-E1 pSer232	Merck	AP1063	1:1000	RRID:AB_10616070
PDH-E1 pSer293	Merck	ABS204	1:5000	RRID:AB_11213668
PDH-E1 pSer300	Merck	ABS194	1:2000	RRID:AB_11204697
PDP1	Sigma-Aldrich	HPA021152	1:5000	RRID:AB_1855635
PDK4	Proteintech	12949-1-AP	1:1000	RRID:AB_2161499
mNCLX (SLC24A6)	Abcam	ab83551	1:500	N/A
VDAC2	Abcam	ab37985	1:2500	RRID:AB_778790
GRP75	Sigma	HPA000898	1:2000	RRID:AB_1079032
TGM2	Sigma	HPA029518	1:3000	N/A
PTPIP51	Sigma	HPA009975	1:2000	RRID:AB_1078811
VAPB	Sigma	HPA013144	1:10000	RRID:AB_1858717
PDZD8	ThermoFischer	PA5-46771	1:500	RRID:AB_2606549
MFN2	Abcam	ab56889	1:2000	RRID:AB_2142629
FIS1	Sigma-Aldrich	HPA017430	1:1000	RRID:AB_1848608
DRP1	CST	#5391	1:1000	RRID:AB_11178938
RyR2	Thermo Fisher	MA3-916	1:1000	RRID:AB_2183054
RyR2 pSer2808	Badrilla	A010-30	1:1000	RRID:AB_2617052
RyR2 pSer2814	Badrilla	A010-31	1:500	RRID:AB_2617055
GAPDH	Santa Cruz	sc-47724	1:80000	RRID:AB_627678
IRDye® 800CW donkey anti-rabbit IgG	Li-Cor	926-32213	1:10000	RRID:AB_621848
IRDye® 800CW donkey anti-goat IgG	Li-Cor	926-32214	1:10000	RRID:AB_621846
IRDye® 680RD donkey anti-mouse IgG	Li-Cor	926-68072	1:10000	RRID:AB_10953628
AzureSpectra 550 goat anti-mouse	Azure Biosystems	512159	1:2500	N/A
STAR 635P anti-rabbit IgG	Abberior	ST635P-1002	1:1000	RRID:AB_2893229
STAR 580 anti-mouse IgG	Abberior	ST580-1001	1:1000	RRID:AB_2923543

Cultured Cells

Name	Vendor or Source	Sex (F, M, or unknown)	Persistent ID / URL
TC-1133	Repairon GmbH	Unknown	RRID:CVCL_RH35
UMGi014-C	University Medical Center Göttingen	Unknown	RRID:CVCL_A4ZE
CRTL1	Healthy donor	F	N/A
WT4	Healthy donor	M	N/A

Other

Description	Source / Repository	Catalog #/Persistent ID / URL
Ezetimibe	Molekula	74798364
Nocodazole	MedChemExpress	HY-13520
Rhod-2 AM	Invitrogen	R1245MP
Indo-1 pentapotassium salt	AAT Bioquest	21040
Fluo-3 AM	AAT Bioquest	21013
Fluo-3 pentapotassium salt	AAT Bioquest	21017
Calcium Green-5N	Invitrogen	C3737
Fluo-4 AM	Invitrogen	F14201
SBFI-AM	Invitrogen	S1264
MitoTracker Orange CMTMRos	Invitrogen	M7510
REVERT™ total protein stain	LI-COR Biotechnology	N/A
RPMI-Glutamax	Gibco	618-70010
B27 supplement	ThermoFischer	17504044
Lipofectamine LTX Reagent with PLUS	Invitrogen	15338100
Karnovsky fixative	Solmedia	HST408S-C
EnVision FLEX Target Retrieval Solution, High pH	Agilent Dako	K8004
EnVision FLEX Wash Buffer	Agilent Dako	K8007
Infinite M200Pro	Tecan	RRID:SCR_019033
PT Link PT200 Autostainer	Agilent Dako	N/A
Oxygraph-2k high-resolution respirometer	Oroboros Instruments	N/A
Leica TCS SP8	Leica	RRID:SCR_018169
Odyssey CLx	LI-COR Biotechnology	RRID:SCR_014579
Fiji	NIH	RRID:SCR_002285
MAXCHELATOR	Stanford University	RRID:SCR_000459
IMOD	University of Colorado	RRID:SCR_003297
MATLAB	Mathworks	RRID:SCR_001622
SPSS	IBM	RRID:SCR_002865

ARRIVE GUIDELINES

The ARRIVE guidelines (<https://arriveguidelines.org/>) are a checklist of recommendations to improve the reporting of research involving animals. Key elements of the study design should be included below to better enable readers to scrutinize the research adequately, evaluate its methodological rigor, and reproduce the methods or findings.

Study Design

Groups	Sex	Age	Number (prior to experiment)	Number (after termination)	Littermates (Yes/No)	Other description
Group 1 (Control)	M	~3 months	3	3	No	N/A
Group 2 (AF)	M	~3 months	3	3	No	N/A

Sample Size

This study was conducted in an exploratory manner to support the primary experimental hypothesis and to reproduce the observations in an animal disease model. Consequently, no formal sample size calculation was undertaken. Instead, the findings were confirmed in three independent animals per group.

Inclusion Criteria

Animals that exhibited sustained AF after a burst pacing protocol were included in the AF group.

Exclusion Criteria

Signs of acute myocardial ischemia or severe infection. Signs of pain or discomfort of the animal, leading the investigators to immediately terminate the experiment.

Randomization and Blinding

Since this large animal study was designed to establish a model for replicating the main hypothesis in an animal disease model, rather than serving as an interventional trial, neither randomization nor blinding was applied.

STROBE Statement—checklist of items that should be included in reports of observational studies

	Item No.	Recommendation	Page No.	Relevant text from manuscript
Title and abstract	1	(a) Indicate the study’s design with a commonly used term in the title or the abstract	Title Page Main Manuscript Page 1	Line 1 Lines 75-79
		(b) Provide in the abstract an informative and balanced summary of what was done and what was found	Main Manuscript Page 1	Lines 75-79
Introduction				
Background/rationale	2	Explain the scientific background and rationale for the investigation being reported	Main Manuscript Pages 2-4	Lines 38-74
Objectives	3	State specific objectives, including any prespecified hypotheses	Main Manuscript Page 4	Lines 75-79
Methods				
Study design	4	Present key elements of study design early in the paper	Main Manuscript Page 1	Lines 1-24
Setting	5	Describe the setting, locations, and relevant dates, including periods of recruitment, exposure, follow-up, and data collection	Supplemental Material 6	Lines 157
Participants	6	(a) Cohort study—Give the eligibility criteria, and the sources and methods of selection of participants. Describe methods of follow-up Case-control study—Give the eligibility criteria, and the sources and methods of case ascertainment and control selection. Give the rationale for the choice of cases and controls Cross-sectional study—Give the eligibility criteria, and the sources and methods of selection of participants	Supplemental Material Page 7	Lines 166-171

		(b) Cohort study—For matched studies, give matching criteria and number of exposed and unexposed Case-control study—For matched studies, give matching criteria and the number of controls per case	Supplemental Material Page 7	Lines 166-171
Variables	7	Clearly define all outcomes, exposures, predictors, potential confounders, and effect modifiers. Give diagnostic criteria, if applicable	Supplemental Material Page 7	Lines 166-171
Data sources/ measurement	8*	For each variable of interest, give sources of data and details of methods of assessment (measurement). Describe comparability of assessment methods if there is more than one group	Supplemental Material Page 7	Lines 166-171
Bias	9	Describe any efforts to address potential sources of bias	Supplemental Material Page 7	Lines 166-171
Study size	10	Explain how the study size was arrived at	Supplemental Material Page 7	Lines 166-171
Quantitative variables	11	Explain how quantitative variables were handled in the analyses. If applicable, describe which groupings were chosen and why	Main Manuscript Page 15-16	Lines 431-442
Statistical methods	12	(a) Describe all statistical methods, including those used to control for confounding	Main Manuscript Pages 6-7 Supplemental Material Pages 33-45	Lines 215-231 Supplemental Statistical Table
		(b) Describe any methods used to examine subgroups and interactions	Supplemental Material Pages 33-45	Supplemental Statistical Table

		(c) Explain how missing data were addressed	Main Manuscript Page 7 Supplemental Material Pages 33-45	Lines 228-230 Supplemental Material Supplemental Statistical Table
		(d) Cohort study—If applicable, explain how loss to follow-up was addressed Case-control study—If applicable, explain how matching of cases and controls was addressed Cross-sectional study—If applicable, describe analytical methods taking account of sampling strategy	N/A	N/A
		(e) Describe any sensitivity analyses	N/A	N/A
Results				
Participants	13*	(a) Report numbers of individuals at each stage of study—eg numbers potentially eligible, examined for eligibility, confirmed eligible, included in the study, completing follow-up, and analysed	Main Manuscript Pages 37-40 Supplemental Material Pages 21-26	Tables 1-2 Supplemental Tables 1-6
		(b) Give reasons for non-participation at each stage	N/A	N/A
		(c) Consider use of a flow diagram	N/A	N/A
Descriptive data	14*	(a) Give characteristics of study participants (eg demographic, clinical, social) and information on exposures and potential confounders	Main Manuscript Pages 37-40 Supplemental Material Pages 21-26	Tables 1-2 Supplemental Tables 1-6
		(b) Indicate number of participants with missing data for each variable of interest	N/A	N/A
		(c) Cohort study—Summarise follow-up time (eg, average and total amount)	N/A	N/A
Outcome data	15*	Cohort study—Report numbers of outcome events or summary measures over time	Main Manuscript Page 52	Figure 6

		Case-control study—Report numbers in each exposure category, or summary measures of exposure	N/A	N/A
		Cross-sectional study—Report numbers of outcome events or summary measures	N/A	N/A
Main results	16	(a) Give unadjusted estimates and, if applicable, confounder-adjusted estimates and their precision (eg, 95% confidence interval). Make clear which confounders were adjusted for and why they were included	Main Manuscript Page 16	Lines 365-368
		(b) Report category boundaries when continuous variables were categorized	N/A	N/A
		(c) If relevant, consider translating estimates of relative risk into absolute risk for a meaningful time period	N/A	N/A

Continued on next page

Other analyses	17	Report other analyses done—eg analyses of subgroups and interactions, and sensitivity analyses	Supplementary Statistical Table	Supplemental Material Pages 33-45
Discussion				
Key results	18	Summarise key results with reference to study objectives	Main Manuscript Page 16	Lines 382-389
Limitations	19	Discuss limitations of the study, taking into account sources of potential bias or imprecision. Discuss both direction and magnitude of any potential bias	Main Manuscript Pages 25-27	Lines 555-602
Interpretation	20	Give a cautious overall interpretation of results considering objectives, limitations, multiplicity of analyses, results from similar studies, and other relevant evidence	Main Manuscript Page 24	Lines 574-580
Generalisability	21	Discuss the generalisability (external validity) of the study results	Main Manuscript Page 25	Lines 589-602
Other information				
Funding	22	Give the source of funding and the role of the funders for the present study and, if applicable, for the original study on which the present article is based	Main Manuscript Page 26	Lines 614-627

*Give information separately for cases and controls in case-control studies and, if applicable, for exposed and unexposed groups in cohort and cross-sectional studies.

Note: An Explanation and Elaboration article discusses each checklist item and gives methodological background and published examples of transparent reporting. The STROBE checklist is best used in conjunction with this article (freely available on the Web sites of PLoS Medicine at <http://www.plosmedicine.org/>, Annals of Internal Medicine at <http://www.annals.org/>, and Epidemiology at <http://www.epidem.com/>). Information on the STROBE Initiative is available at www.strobe-statement.org.